

1 **Biogeochemical processes captured by carbon isotopes in**
2 **redox-stratified water columns: a comparative study of four**
3 **modern stratified lakes along an alkalinity gradient.**
4

Supprimé: A

Supprimé: isotopic

Supprimé: the biogeochemical cycle of carbon in

Supprimé: redox-

Mis en forme : Non Barré

5 Robin Havas^{a,*}, Christophe Thomazo^{a,b}, Miguel Iniesto^c, Didier Jézéquel^d, David Moreira^c, Rosaluz Tavera^e,
6 Jeanne Caumartin^f, Elodie Muller^f, Purificación López-García^c, Karim Benzerara^f

7
8 ^a Biogéosciences, CNRS, Université de Bourgogne Franche-Comté, 21000 Dijon, France

9 ^b Institut Universitaire de France, 75005 Paris, France

10 ^c Ecologie Systématique Evolution, CNRS, Université Paris-Saclay, AgroParisTech, 91190 Gif-sur-Yvette,
11 France

12 ^d IPGP, CNRS, Université de Paris, 75005 Paris, and UMR CARRTEL, INRAE & USMB, France

13 ^e Departamento de Ecología y Recursos Naturales, Universidad Nacional Autónoma de México, México

14 ^f Sorbonne Université, Muséum National d'Histoire Naturelle, CNRS, Institut de Minéralogie, de Physique des
15 Matériaux et de Cosmochimie (IMPMC), 75005 Paris, France.

16
17
18 * Correspondence to: Robin Havas (robin.havas@gmail.com)

Code de champ modifié

19
20
21
22
23 *Keywords:* Carbon cycle; DIC; POC; isotopic fractionation; Precambrian *analogues*,
24

Supprimé: analogs

30 **Abstract.** Redox-stratified water columns are a prevalent feature of Earth history, and ongoing environmental
31 changes tend to promote a resurgence of such settings. Studying modern redox-stratified environments has
32 improved our understanding of biogeochemical processes and element cycling in such water columns. These
33 settings are associated with peculiar carbon biogeochemical cycling owing to a layered distribution of biological
34 processes in relation to oxidant availability. These processes and their sedimentological expression, notably
35 inferred from paired organic matter–carbonate isotopic compositions of carbon, can vary from one stratified
36 environment to another, because metabolisms from different biogeochemical layers are diverse and may differently
37 imprint the sedimentological record. This variability can arise from numerous physico-chemical parameters, such
38 as sedimentation rate, pH, trace element availability, or basin physiography. Changes in the organic/inorganic
39 carbon sources and mass balance can further complicate the isotopic message in these systems. Better
40 understanding of these multifaceted carbon isotope signals requires further evaluation of the transfer function from
41 the processes occurring in redox-stratified water columns to sediments. We therefore characterized and compared
42 the isotopic signatures of carbonate, organic matter, and dissolved inorganic carbon (DIC) reservoirs at different
43 depths in the water column and upper sediments of four stratified Mexican lakes that follow a gradient of
44 alkalinity/salinity. Comparing these systems shows strong diversity in both the water column and sedimentary
45 carbon isotope signals. Differences in inorganic carbon isotope signatures arise primarily from the size of the DIC
46 reservoirs, buffering the expression of redox-dependent biological processes as alkalinity increases. Combining
47 this isotopic dataset with physico-chemical parameters of the water columns allows us to identify the activity of
48 oxygenic photosynthesis and aerobic respiration in the four lakes studied, while anoxygenic photosynthesis is
49 evidenced in two of them. However, sedimentary organic matter does not originate from the same water column
50 layers in the four lakes, highlighting the ecological variability that can stem from distinct stratified water columns
51 and how it is transferred to the sedimentary record. The least alkaline lake shows higher isotopic variability, and
52 signatures typical of methanogenesis in the sediment porewaters. This metabolism, however, does not leave
53 diagnostic isotopic signatures in the sedimentary archives (organic matter and carbonates), underlining the fact
54 that even when alkalinity does not strongly buffer the inorganic carbon reservoir, a comprehensive picture of the
55 active biogeochemical carbon cycling is not necessarily transferred to the geological record.

Supprimé: Abstract. The carbon cycle is central to the evolution of biogeochemical processes at the surface of the Earth. Understanding the interplay between the C cycle and physico-chemical and biological conditions in ancient times is challenging because of major differences between the modern and the ancient Earth. Notably, the atmosphere was less oxidizing and the oceans were redox-stratified. Here, we characterized and compared the C cycles in four redox-stratified alkaline lakes from Mexico based on the concentrations and isotopic compositions of dissolved inorganic and particulate organic C (DIC and POC). Measurements were performed in both the water columns and surficial bottom sediments with the assessment of their physico-chemical parameters (conductivity, temperature, O₂, Chl. a, turbidity,). The four lakes exhibit a range of DIC concentrations from 7 to 35 mM, following a gradient of alkalinity/salinity. The DIC and sedimentary carbonates isotopic compositions ($\delta^{13}\text{C}_{\text{DIC}}$, $\delta^{13}\text{C}_{\text{carb}}$) also varied correlatively with alkalinity increasing from -4.1 to +2.0 ‰ and -1.5 to +4.7 ‰, respectively. The porewaters $\delta^{13}\text{C}_{\text{DIC}}$ reaches up to ~10 ‰ in the sediment of one of the lakes. The $\delta^{13}\text{C}_{\text{POC}}$ varies from -29.0 to -23.5 ‰ in both the water columns and sediments of the four lakes. The depth profiles of $\delta^{13}\text{C}_{\text{POC}}$, [POC] and C:N of organic matter shows very similar variations among three of the lakes located in the same area. From the inter-comparison of these datasets in four different systems, we identify the impact of external abiotic factors such as the hydrological regime and inorganic C sources which control the alkalinity, carbonate isotopic signatures, and stratification of some of the physico-chemical parameters. We identify the presence of oxygenic photosynthesis and aerobic respiration metabolisms in the four lakes as well as of methanogenesis in the one with extreme porewater $\delta^{13}\text{C}_{\text{DIC}}$. Anoxygenic photosynthesis and/or chemoautotrophy are also recognized in two of the lakes, but their POC and DIC signatures can be equivocal. Finally, we find that geochemical signatures of OC in the surficial sediments do not always record the same part of the stratified water column and can be altered by early diagenesis, whereas recently deposited carbonates are more consistently recording the lakes oxycline isotopic compositions. Overall, this work highlights how the integration of datasets from multiple environments facilitates our understanding of the processes affecting the C cycle in redox-stratified systems, while showing the versatility of these processes and how they are recorded in the sedimentary archives.

-----Saut de page-----

105 1. INTRODUCTION

106 The carbon cycle and biogeochemical conditions prevailing at the surface of the Earth are intimately bound through
107 biological (e.g. photosynthesis) and geological processes (e.g. volcanic degassing and silicate weathering). The
108 analysis of carbon isotopes in organic matter and carbonates ($\delta^{13}C_{org}$ and $\delta^{13}C_{carb}$) in the rock record, has been used
109 to reconstruct the evolution of the biosphere and the oxygenation of the Earth's surface (e.g. Hayes et al., 1989;
110 Karhu and Holland, 1996; Schidlowski, 2001). Coupling $\delta^{13}C_{org}$ - $\delta^{13}C_{carb}$ has frequently been used to infer the burial
111 rate of organic C, and thus the redox balance of the atmosphere and hydrosphere (e.g. Karhu and Holland, 1996;
112 Aharon, 2005; Krissansen-Totton et al., 2015; Mason et al., 2017). It has also been used to deduce the presence of
113 metabolisms like anoxygenic chemoautotrophic or methanotrophic bacteria (e.g. Hayes et al., 1999; Bekker et al.,
114 2008; Krissansen-Totton et al., 2015). Coupling $\delta^{13}C_{org}$ - $\delta^{13}C_{carb}$ has also been used to discuss oceans stratification
115 and its effect on inorganic and organic C geochemical signatures in sediments (e.g. Logan et al., 1995; Aharon,
116 2005; Bekker et al., 2008; Ader et al., 2009). Stratification favors the expression and recording of different layers
117 of the water column, with potentially very distinct isotopic signatures. As the oceans were redox-stratified during
118 most of the Earth's history (Lyons et al., 2014; Havig et al., 2015; Satkoski et al., 2015), processes affecting the C
119 cycle were likely different from those occurring in most modern, well-oxygenated environments. This change of
120 conditions could impact the $\delta^{13}C_{org}$ signal at various scales, from changes in diversity and relative abundance of
121 microbial carbon and energy metabolism (e.g. Wang et al., 2016; Iñiguez et al., 2020; Hurley et al., 2021), to larger
122 ecological interactions (e.g. Jiao et al., 2010; Close and Henderson, 2020; Klawonn et al., 2021) and global C
123 dynamics (e.g. Ridgwell and Arndt, 2015; Ussiri and Lal, 2017).

124 Modern stratified lakes have been used as analogues of ancient redox-stratified systems to better understand the C
125 cycle in the sedimentary isotopic record (e.g. Lehmann et al., 2004; Posth et al., 2017; Fulton et al., 2018). Several
126 number of recent studies have investigated the C cycle in modern stratified water columns (e.g. Crowe et al., 2011;
127 Kuntz et al., 2015; Posth et al., 2017; Schiff et al., 2017; Havig et al., 2018; Cadeau et al., 2020; Saini et al., 2021;
128 Petrash et al., 2022), where many bio-geo-physico-chemical parameters can be directly measured, together with
129 the main C reservoirs. However, investigations of such Precambrian analogues do not necessarily include sediment
130 data, and generally focus on a single environment without integrating views from several systems.

131 In this study, we measured the concentrations and isotopic compositions of dissolved inorganic carbon (DIC) and
132 particulate organic carbon (POC) throughout the water column of four modern redox-stratified alkaline crater
133 lakes, located in the Trans-Mexican Volcanic Belt (Ferrari et al., 2012). We also measured the concentrations and
134 isotopic compositions of the sedimentary organic carbon and carbonates as well as porewater DIC from surficial
135 sediments (~ 10 cm) at the bottom of the lakes. The four lakes share similar geological and climatic contexts but
136 have distinct solution chemistries along a marked alkalinity-salinity gradient (Zeyen et al., 2021) – as well as
137 distinct planktonic communities (Iniesto et al., 2022). We therefore seek to evaluate how these environmental and
138 ecological differences are recorded in the C isotope signatures in the water columns (DIC-POC) and sedimentary
139 archives (organic matter-carbonates). The four lakes are closed lakes in endorheic basins (Alcocer, 2021; Zeyen
140 et al., 2021), which facilitates the identification of external environmental constraints (e.g. evaporation, C sources)
141 and their influence on processes occurring within the water columns. Depth profiles of the main physico-chemical
142 parameters together with trace and major elements concentrations were measured to pinpoint the dominant
143 biogeochemical processes occurring in the water columns and link them to specific C isotopes signatures.

- Mis en forme : Police :Non Italique
- Supprimé : ,
- Mis en forme : Police :Non Italique
- Supprimé: Accordingly, the
- Supprimé: the
- Mis en forme : Police :Non Italique
- Supprimé: Hayes et al., 1989; Karhu and Holland, 1996; Schidlowski, 2001; Bekker et al., 2008). However, because the oceans have been
- Supprimé: throughout
- Code de champ modifié
- Supprimé:
- Supprimé: Indeed, while biological processes evolved (...)
- Supprimé: C cycle
- Supprimé: diverse
- Supprimé: starting
- Supprimé: the
- Supprimé: (e.g. Wang et al., 2016; Iñiguez et al., 2020; (...)
- Mis en forme (...)
- Mis en forme (...)
- Supprimé: Nonetheless, some modern
- Supprimé: analogs (anoxic at depth) of early oceans exist (...)
- Supprimé: and how it was recorded by
- Supprimé: archives
- Mis en forme (...)
- Code de champ modifié (...)
- Supprimé: To this end, a
- Supprimé: of
- Mis en forme (...)
- Supprimé: Crowe et al., 2011; Kuntz et al., 2015; Camach (...)
- Supprimé: of their
- Supprimé: could
- Supprimé: these
- Supprimé: the C cycle in
- Supprimé: usually
- Supprimé: instead of
- Supprimé: (e.g. Camacho et al., 2017; Schiff et al., 2017).
- Supprimé: Here
- Supprimé: propose to describe
- Supprimé: C cycle
- Supprimé: trans
- Supprimé: volcanic belt
- Supprimé: . For this purpose, we measured the (...)
- Déplacé (insertion) [1]

206 ~~First, we constrain the main DIC sources and external controls on the lakes' alkalinity. Next, we describe the~~
207 ~~influence of the inter-lake alkalinity gradient on the inorganic C cycle and stratification of the lakes, and how it is~~
208 ~~recorded in surficial sediments. Then, by combining POC and DIC data, we identify the sources of organic C to~~
209 ~~the lakes by describing the main autotrophic reactions occurring in the water columns (e.g. oxygenic and~~
210 ~~anoxygenic photosynthesis). Finally, we discuss the fate of POC, either recycled (e.g. via methanogenesis) or~~
211 ~~deposited in the sediments, and how all these processes are recorded (or not) in surficial sediments.~~

212

213 2. SETTING / CONTEXT

214 2.1. Geology

215 The four lakes studied here are volcanic maars formed after phreatic, magmatic, and phreatomagmatic explosions,
216 ~~related to~~ volcanic activity in the Trans-Mexican Volcanic Belt (TMVB, Fig. 1). ~~The~~ TMVB originates from the
217 subduction of the Rivera and Cocos plates beneath the North America plate, resulting in a long (~~~1000 km~~) and
218 wide (~~90-230 km~~) Neogene volcanic arc spreading across central Mexico (Ferrari et al., 2012). The TMVB harbors
219 a large variety of monogenetic scoria cones ~~and phreatomagmatic vents (maars and tuff-cones)~~ as well as
220 stratovolcanoes, calderas, and domes (Carrasco-Núñez et al., 2007; Ferrari et al., 2012; Siebe et al., 2014). Maar
221 crater formation usually occurs when ascending ~~magma meets~~ water-saturated substrates, leading to successive
222 explosions and ~~the~~ excavation of older units (Lorenz, 1986; Carrasco-Núñez et al., 2007; Siebe et al., 2012; Chako
223 Tchamabé et al., 2020).

224 ~~The first lake, La Alberca de los Espinos (1985 masl), is located at the margin of the Zacapu tectonic lacustrine~~
225 ~~basin in the Michoacán-Guanajuato Volcanic Field (MGVF) in the central-western part of the TMVB (Fig. 1). It~~
226 ~~lies on andesitic basement rocks and was dated at $\sim 25 \pm 2$ ka (Siebe et al., 2012, 2014). The other three lakes (La~~
227 ~~Preciosa, Atexcac and Alchichica) are all in the same area (~ 50 km²) of the Serdan-Oriental Basin (SOB) in the~~
228 easternmost part of the TMVB (Fig. 1). The SOB is a closed intra-montane basin at high altitude (~ 2300 m),
229 surrounded by the Los Humeros caldera ~~to~~ the north and the Cofre de Perote-Citlatépel volcanic range ~~to~~ the east.
230 The basement is ~~composed of~~ folded and faulted Cretaceous limestones and shales, covered by andesitic ~~to~~ basaltic
231 lava flows (Carrasco-Núñez et al., 2007; Armienta et al., 2008; Chako Tchamabé et al., 2020). The Alchichica and
232 Atexcac craters ~~was~~ dated ~~at~~ $\sim 6-13 \pm 5-6$ ka (Chako Tchamabé et al., 2020) and 330 ± 80 ka (Carrasco-Núñez et
233 al., 2007), ~~respectively~~ (Table 1). ~~The age of~~ La Preciosa is not known.

234

235 2.2. Climate and limnology

236 ~~La Alberca is a freshwater lake (0.6 psu) with a temperate to semi-humid climate (Rendon-Lopez, 2008; Sigala et~~
237 ~~al., 2017). In contrast,~~ lakes from the SOB experience a similar temperate to semi-arid climate (Armienta et al.,
238 2008; Sigala et al., 2017). The ~~current~~ climate of the SOB is dominated by dry conditions, ~~reflected by~~ higher
239 evaporation than precipitation fluxes in Lake Alchichica (~ 1686 vs 392 mm/year; Alcocer, 2021). ~~In~~ La Preciosa,
240 ~~Atexcac, and Alchichica,~~ this trend is reflected by a drop in water level evidenced by the emersion of microbialite
241 deposits (Fig. S1; Zeyen et al., 2021). This evaporation-dominated climate strongly contributes to the ~~relatively~~
242 high salinity values in these lakes ($1.2-7.9$ psu), ranging from sub- to hyposaline.

Supprimé: The four lakes share similar geological and climatic contexts but have distinct solution chemistries (Zeyen et al., 2021)

Déplacé vers le haut [1]: - as well as distinct planktonic communities (Iniesto et al., 2022).

Supprimé: Overall, their inter-comparison via the same methodology allows to assess the effects of specific physico-chemical and biological parameters on the C cycle. Moreover, they all correspond to closed lakes in endorheic basins

Mis en forme : Couleur de police : Noir

Supprimé: in relation with

Supprimé: -

Supprimé: (~ 1000 and

Supprimé: -

Supprimé: , respectively

Supprimé: phreatomagmatic vents (maars and

Supprimé: magmas meet

Supprimé: Three of the studied

Déplacé (insertion) [2]

Supprimé: Alchichica

Supprimé: La Preciosa

Supprimé: located

Supprimé: a restricted

Supprimé: in

Supprimé: in

Supprimé: mainly

Supprimé:

Supprimé:

Supprimé: formations of

Supprimé: were

Supprimé: back to

Supprimé: ka, respectively (Table 1; Carrasco-Núñez et al.)

Supprimé: The fourth lake, La Alberca de los Espinos, is

Déplacé vers le haut [2]: on andesitic basement rocks and

Supprimé: Due

Supprimé: their geographical proximity

Supprimé: present

Supprimé: as

Supprimé: In Alchichica, Atexcac and

Supprimé: their

Supprimé: in these lakes

Supprimé: achievement of

Supprimé: lake salinities from

Supprimé: to

Supprimé: ,

Supprimé: In comparison, La Alberca's climate is temper

319 The four lakes are warm monomictic; they are stratified for about nine months of the year, mixing only when
320 thermal stratification breaks down in the cold of winter (Armentia et al., 2008). They are all closed lakes located
321 in an “endorheic” basin (Alcocer, 2021; Zeyen et al., 2021), meaning that they have no inflow, outflow, or
322 connection to other basins through surficial waters such as streams. The only water input is from precipitation and
323 groundwater inflow (quantified for Lake Alchichica; (Alcocer, 2021 and references therein).

324 The four lakes are alkaline (pH ~ 9) but cover a broad range of chemical compositions (including alkalinity,
325 salinity, and Mg/Ca ratio), interpreted as reflecting different concentration stages of an initial alkaline dilute water
326 (Table 1; Zeyen et al., 2021). Variations in concentration stages may be due to differences in climate, and, more
327 generally, different hydrological regimes. Microbialite deposits are found in all four lakes (Gérard et al., 2013;
328 Saghaï et al., 2016; Iniesto et al., 2021a, 2021b; Zeyen et al., 2021), and increase in abundance from lower to
329 higher alkalinity conditions (Zeyen et al., 2021).

330

331 3. METHOD

332 3.1. Sample Collection

333 The sediment core from Lake La Preciosa was collected in May 2016. All other samples were collected in May
334 2019. The depth profiles of several physico-chemical parameters were measured in the water columns of the four
335 lakes using an YSI Exo 2 multi-parameter probe: temperature, pH, ORP (oxidation reduction potential),
336 conductivity, O₂, chlorophyll a, phycocyanin, and turbidity. Precisions for these measurements were 0.01 °C, 0.1
337 pH unit, 20 mV, 0.001 mS/cm, 0.1 mg/L, 0.01 µg/L, 0.01 µg/L and 2% FTU unit, respectively. The ORP signal
338 was not calibrated before each profile and is thus used to discuss relative variations over a depth profile.

339 Measurements of the aforementioned parameters served to pinpoint depths of interest for further chemical and
340 isotopic analyses, notably around the redoxcline of the lakes. Water samples were collected with a Niskin bottle.
341 Particulate matter was collected on pre-combusted (2 h at 490°C) and weighted glass fiber filters (Whatman GF/F,
342 0.7 µm) and analyzed for particulate organic carbon (POC), major and trace elements. Between 1.5 and 5 L of lake
343 water was filtered before the GF/F filters became clogged. The processed solution was filtered again at 0.22 µm
344 with Filtropur S filters (pre-rinsed with lake water filtered at 0.7 µm) for analyses of dissolved inorganic carbon
345 (DIC), and major, minor, and trace ions.

346 Sediment cores were collected using a 90 mm Uwitec corer close to the deepest point of each lake’s water column
347 (Table 1), where anoxic conditions prevail almost all year long. Cores measured between 20 and 85 cm in length.
348 Slices of about 2-3 cm were cut under anoxic conditions, using a glove bag filled with N₂ (anoxia was monitored
349 using a WTW3630 equipped with a FDO O₂ optode). Interstitial porewater was drained out of the core slices using
350 Rhizons in the glove bag. Sediments were transported back to the laboratory within aluminized foils (Protpack,
351 UK). Sediments were then fully dried in a laboratory anoxic N₂-filled glove box.

352

Supprimé: , i.e.,

Supprimé: throughout most

Supprimé: (~ 9 months) and mix once a year

Supprimé: the

Supprimé: “

Supprimé: ”

Supprimé: i.e.

Supprimé: nor a

Supprimé: Overall,

Supprimé: only supplied by precipitations

Supprimé: as evidenced and

Supprimé: Finally, the

Supprimé: distribute over

Supprimé: gradient

Supprimé: varying

Supprimé: concentrations

Supprimé: different climates (mostly between La Alberca

Supprimé: lakes from the SOB) and

Supprimé: with an increasing

Supprimé: alkaline

Supprimé:

Supprimé: allowed

Supprimé: were

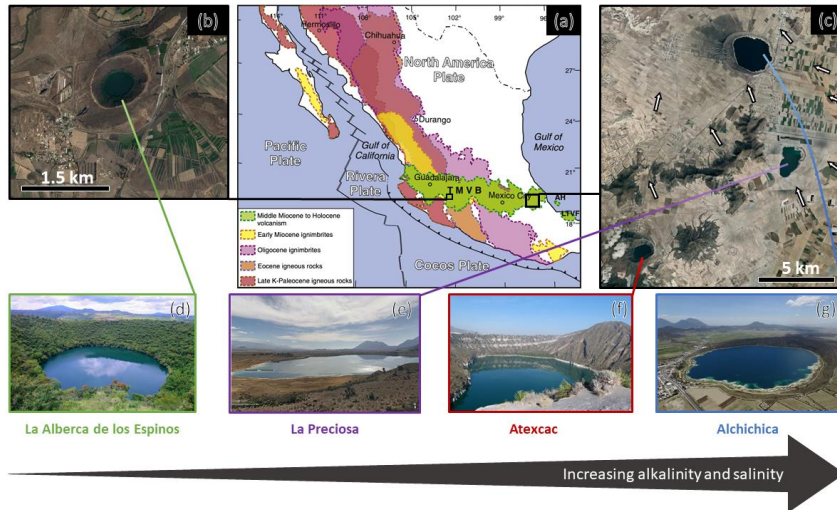
Supprimé: got

Supprimé: Then,

Supprimé: that were

Supprimé: the

Supprimé: were



381 Figure 1. Geographical location and photographs of the **four** crater lakes. (a) Geological map from Ferrari et al.
 382 (2012) **with black squares showing** the location of the four studied lakes **within the Trans-Mexican Volcanic Belt**
 383 (TMVB). (b, c) Close up © Google Earth views of **La Alberca de los Espinos** and the **Serdan-Oriental Basin**
 384 (SOB). **The white arrows represent the approximate groundwater flow path** (based on Silva-Aguilera, 2019). (d-
 385 g) **Photographs** of the four lakes (d from © Google Image [*'enamoratedemexicowebiste'*], e from © Google Earth
 386 street view, and g from © *'Agencia Es Imagen'*).

388

Lake	General location	Sampling location	Elevation (masl)
<u>Alchichica</u>	<u>Serdan Oriental Basin,</u> <u>eastern TMVB</u>	<u>19°24'51,5" N;</u> <u>97°24'09,9" W</u>	<u>2320</u>
<u>Atexcac</u>	<u>Serdan Oriental Basin,</u> <u>eastern TMVB</u>	<u>19°20'2.2" N;</u> <u>97°26'59.3" W</u>	<u>2360</u>
<u>La Preciosa</u>	<u>Serdan Oriental Basin,</u> <u>eastern TMVB</u>	<u>19°22'18.1" N;</u> <u>97°23'14.4" W</u>	<u>2330</u>
<u>La Alberca de los Espinos</u>	<u>Zacapu Basin, MGVF,</u> <u>central TMVB</u>	<u>19°54'23.9" N;</u> <u>101°46'07.8" W</u>	<u>1985</u>

389

Lake	Lake Basement	Age	Max Depth (m)	Alkalinity (mmoles/L)	Salinity (psu)	pH
<u>Alchichica</u>	<u>limestone, basalts</u>	<u>6-13 ± 5-6 ka</u>	<u>63</u>	<u>~35</u>	<u>7.9</u>	<u>9.22</u>
<u>Atexcac</u>	<u>limestone, andesites,</u> <u>basalts</u>	<u>330 ± 80 ka</u>	<u>39</u>	<u>~26</u>	<u>7.4</u>	<u>8.85</u>
<u>La Preciosa</u>	<u>limestone, basalts</u>	<u>Pleistocene</u>	<u>46</u>	<u>~13.5</u>	<u>1.15</u>	<u>9.01</u>
<u>La Alberca de los Espinos</u>	<u>andesite xenoliths</u>	<u>25 ± 2 ka</u>	<u>30</u>	<u>~7</u>	<u>0.6</u>	<u>9.14</u>

390

391 Table 1. General information about the **lakes** studied. Abbreviations: TMVB: Trans-Mexican **Volcanic Belt**;
 392 MGVF: Michoacán-Guanajuato **Volcanic Field**; **masl**: meters above sea level. **NB**: Sampling **took place** in
 393 May 2019, except for La **Preciosa**, sediments, sampled in May 2016.

Mis en forme : Police :+Corps (Calibri), 11 pt

Supprimé: studied

Mis en forme : Police :10 pt

Mis en forme : Police :10 pt

Supprimé: representing

Mis en forme : Police :10 pt

Supprimé: in

Mis en forme : Police :10 pt

Supprimé: trans

Mis en forme : Police :10 pt

Supprimé: volcanic belt

Mis en forme : Police :10 pt

Supprimé:), (

Mis en forme : Police :10 pt

Supprimé: lake

Mis en forme : Police :10 pt

Mis en forme : Police :10 pt

Mis en forme : Police :10 pt

Supprimé:), respectively.

Mis en forme : Police :10 pt

Supprimé: Pictures

Mis en forme : Police :10 pt

Supprimé: studied

Mis en forme : Police :10 pt

Mis en forme : Police :10 pt

Mis en forme : Police :10 pt

Mis en forme : Police :10 pt

Mis en forme : Police :10 pt

Mis en forme : Police :10 pt

Mis en forme : Police :10 pt

Mis en forme : Police :10 pt

Supprimé: Lake

Mis en forme : Police :10.5 pt

Supprimé: lakes

Supprimé: volcanic belt

Supprimé: volcanic field; m.a.s.l

Supprimé: Preciosa's

409 **3.2. Dissolved inorganic carbon (DIC) concentration and isotope measurements**

410 Twelve mL of the 0.7-µm filtered lake water was filtered at 0.22-µm directly into hermetic Exetainer® tubes to
411 avoid exchange between DIC and atmospheric CO₂. The DIC concentrations and isotopic compositions were
412 measured at the Institut de Physique du Globe de Paris (IPGP, France), using an Analytical Precision 2003 GC-
413 IRMS, running under He-continuous flow, following the protocol described by Assayag et al. (2006). A given
414 volume of the solution was extracted from the Exetainer® tube with a syringe, while the same volume of helium
415 was introduced to maintain stable pressure and atmospheric-CO₂-free conditions within the sample tubes. The
416 collected sample was inserted into another Exetainer® tube, pre-filled with a few drops of 100% phosphoric acid
417 (H₃PO₄) and pre-flushed with He gas. Under acidic conditions, DIC quantitatively converts to gaseous and aqueous
418 CO₂, which equilibrates overnight within the He-filled head space of the tube. Quantification and isotopic analyses
419 of released gaseous CO₂ were then carried out by GC-IRMS using internal standards of known composition that
420 were prepared and analyzed via the same protocol. Each measurement represented an average of four injections in
421 the mass spectrometer. Chemical preparation and IRMS analysis were duplicated for all the samples. The δ¹³C_{DIC}
422 reproducibility calculated for the 65 samples was better than ±0.2 ‰, including internal and external
423 reproducibility. Standard deviation for [DIC] was 0.6 ± 0.9 mmol/L on average.

424 Specific DIC speciation, i.e., CO_{2(aq)}, HCO₃⁻ and CO₃²⁻ activities, was computed using Phreeqc with the full
425 dissolved chemical composition of each sample as an input. It should be noted that these results are calculated
426 from theoretical chemical equilibria and do not necessarily take into account local kinetic effects, which, for
427 example, could lead to local exhaustion of CO_{2(aq)} where intense photosynthesis occurs.

428

429 **3.3. Particulate organic carbon and nitrogen (POC / PON)**

430 Particulate organic matter from the lake water columns was collected on GF/F filters, dried at room temperature
431 and ground in a ball mill before and after decarbonation. Decarbonation was performed with 12N HCl vapors in a
432 desiccator for 48 h. Aliquots of dry decarbonated samples (25 - 70 mg) were weighed in tin capsules. The POC
433 and PON contents and δ¹³C_{POC} were determined at the Laboratoire Biogéosciences (Dijon, France) using a Vario
434 MICRO cube elemental analyzer (Elementar, Hanau, Germany) coupled in continuous flow mode with an
435 IsoPrime IRMS (Isoprime, Manchester, UK). The USGS 40 and IAEA 600 certified materials used for calibration
436 showed reproducibility better than 0.15 ‰ for δ¹³C. External reproducibility based on triplicate analyses of
437 samples (n=23) was 0.1 ‰ on average for δ¹³C_{POC} (1SD). External reproducibility for POC and PON
438 concentrations was 0.001 and 0.005 mmol/L on average, respectively (i.e. 3 and 7 % of measured concentrations).

439

440 **3.4. Geochemical characterizations of the sediments**

441 Sedimentary organic carbon (SOC), sedimentary organic nitrogen (SON), and their isotopic compositions were
442 measured on carbonate-free residues of the first 12 cm of the sediment cores, produced after overnight 1N HCl
443 digestion. Plant debris (mainly found in La Alberca and Atexcac) was identified upon initial sediment grinding in
444 an agate mortar and analyzed separately. Aliquots of dried decarbonated samples (~ 4-70 mg) were weighed in tin
445 capsules. The SOC and SON contents and δ¹³C were determined at the Laboratoire Biogéosciences (Dijon) using

- Supprimé: milliliters
- Supprimé: were
- Supprimé: in order
- Supprimé: and
- Supprimé: In short, a
- Supprimé: is taken out of
- Supprimé: is
- Supprimé: in order
- Supprimé: a
- Supprimé: is introduced in
- Supprimé: that was
- Supprimé: the
- Supprimé:
- Supprimé: are
- Supprimé: represents
- Mis en forme : Police :Non Italique
- Supprimé: provided by calculations of
- Supprimé: were
- Supprimé: and
- Supprimé: a
- Supprimé: reproducibilities of
- Supprimé: were on average
- Mis en forme : Police :Non Italique
- Mis en forme : Hiérarchisation + Niveau : 2 + Style de numérotation : 1, 2, 3, ... + Commencer à : 1 + Alignement : Gauche + Alignement : 0 cm + Retrait : 0.63 cm
- Supprimé: ¶
Sedimentary organic carbon (SOC), sedimentary organic nitrogen (SON) and their isotopic compositions were measured on carbonate-free residues of the first 12 cm of the sediment cores, produced after overnight 1N HCl digestion (...)
- Déplacé vers le bas [3]: upon initial sediment grinding
- Déplacé vers le bas [4]: SOC and SON contents and δ¹³C
- Supprimé: USGS 40 and IAEA 600 certified materials (...)
- Déplacé vers le bas [5]: Sample analyses (n=67) were at
- Supprimé: External reproducibilities for SOC and SON (...)
- Déplacé vers le bas [6]: were analyzed at the Laboratoire
- Supprimé: Carbonate total
- Déplacé vers le bas [7]: concentration was determined
- Supprimé: Minerals identification were based on COD (...)
- Déplacé vers le bas [8]: after a wet chemical extraction
- Mis en forme : Police :Non Italique
- Déplacé (insertion) [3]
- Déplacé (insertion) [4]

533 a Vario MICRO cube elemental analyzer (Elementar GmbH, Hanau, Germany) coupled in continuous flow mode
 534 with an IsoPrime IRMS (Isoprime, Manchester, UK). The USGS 40 and IAEA 600 certified materials used for
 535 calibration had a reproducibility better than 0.2 ‰ for $\delta^{13}\text{C}_{\text{SOC}}$. Sample analyses (n=67) were at least duplicated
 536 and showed an average external reproducibility of 0.1 ‰ for $\delta^{13}\text{C}$ (1SD). External reproducibility for SOC and
 537 SON contents was 0.1 and 0.03 wt. %, respectively.

538 Carbon isotope compositions of sedimentary carbonates were analyzed at the Laboratoire Biogéosciences (Dijon)
 539 using a ThermoScientific™ Delta V Plus™ IRMS coupled with a Kiel VI carbonate preparation device. External
 540 reproducibility was assessed by multiple measurements of NBS19 standard and was better than ± 0.1 ‰ (2σ).
 541 Total carbonate concentration was determined by mass balance after decarbonation for SOC analysis.

542 Mineralogical assemblages of sediments were determined on bulk powders by X-Ray diffraction (XRD) at the
 543 Laboratoire Biogéosciences (Dijon). Samples were ground in an agate mortar. Diffractograms were obtained with
 544 a Bruker D8 Endeavor diffractometer with $\text{CuK}\alpha$ radiation and LynxEye XE-T detector, under 40 kV and 25 mA
 545 intensity. Mineral identification was based on COD (“Crystallography Open Database”) and BGMN databases.
 546 Mineral abundances were estimated by Rietveld refinement analysis implemented in the Profex software.

547 Solid sulfide concentrations were determined on dry bulk sediments from La Alberca Lake after a wet chemical
 548 extraction using a boiling acidic Cr(II)-solution as detailed in Gröger et al. (2009).

549

550 3.5. Major and trace elements concentrations

551 Dissolved and particulate matter elemental compositions were measured at the Pôle Spectrométrie Océan
 552 (Plouzané, France) by inductively coupled plasma-atomic emission spectroscopy (ICP-AES, Horiba Jobin) for
 553 major elements and by high-resolution ICP-mass spectrometry using an Element XR (HR-ICP-MS, Thermo Fisher
 554 Scientific) for trace elements. Major element measurement reproducibility based on internal multi-elemental
 555 solution was better than 5%. Trace elements were analyzed by a standard-sample bracketing method and calibrated
 556 with a multi-elemental solution. Analytical precision for trace elements was generally better than 5%. Dissolved
 557 sulfate concentrations were analyzed by ion chromatography at the IPGP (Paris, France) with uncertainty lower
 558 than 5%.

559

560 4. RESULTS

561

562 4.1. Lake La Alberca de los Espinos

563 Stratification of the water column was well defined in La Alberca de los Espinos (Fig. 2). Temperature was higher
 564 than in the other lakes (decreasing from ~ 23 °C at the surface to 16.5 °C at depth). Dissolved O_2 was oversaturated
 565 at the lake surface (118 %, i.e., 7.9 mg/L), rapidly decreasing to 0 between ~ 5 and 12 m, while the oxidation
 566 reduction potential (ORP) only decreased below 17 m depth. The offset between O_2 exhaustion and ORP decrease
 567 can be explained by the presence of other oxidant species and/or extended chlorophyll a peaks (supplementary
 568 text 1). Conductivity decreased from 1.20 to 1.17 mS/cm at 16 m before increasing to 1.27 mS/cm at 26 m (salinity

Déplacé (insertion) [5]

Déplacé (insertion) [6]

Déplacé (insertion) [7]

Déplacé (insertion) [8]

Supprimé:

Supprimé: -mass

Supprimé:

Supprimé: -

Supprimé: -

Supprimé: an

Déplacé vers le bas [9]: <#>Lake Alchichica¶
 <#>The water column of Lake Alchichica showed a pronounced stratification compared to previous years at the same period (Fig. 2, Fig. S2; Lugo et al., 2000; Adame et al., 2008; Macek et al., 2020).

Supprimé: <#>The water temperature varied from about 20 °C at the surface to 15.5 °C at a 30 m depth and below. (...)

Déplacé vers le bas [10]: <#> pH remained constant at

Supprimé: <#> 2).¶ (...)

Déplacé vers le bas [11]: <#> The $\delta^{13}\text{C}_{\text{DIC}}$ decreased

Supprimé: <#>2). Calculated pCO_2 was about three time (...)

Déplacé vers le bas [12]: <#>Lake Atexcac¶

Supprimé: <#>Temperature was about 20.6 °C at the (...)

Déplacé vers le bas [13]: <#> Turbidity showed a

Supprimé: <#>Finally, pH remained around 8.85 (...)

Déplacé vers le bas [14]: <#> $\delta^{13}\text{C}_{\text{POC}}$ showed minimum

Supprimé: <#>Dissolved sulfate concentration was (...)

Déplacé vers le bas [15]: <#>¶

Mis en forme : Non souligné

Supprimé: <#>The temperature varied from about 20 °C (...)

Déplacé vers le bas [16]: <#>Dissolved O_2 was

Mis en forme : Police :Non Italique

Supprimé: <#>8.4 mg/L) and rapidly decreased to 0 (...)

Déplacé vers le bas [17]: <#> and recorded the highest

Supprimé: <#>Finally, pH showed a small decrease from (...)

Déplacé vers le bas [18]: <#>2).¶

Supprimé: <#>2). Calculated pCO_2 at the surface (...)

Déplacé vers le bas [19]: <#>. The $\delta^{13}\text{C}_{\text{DIC}}$ decreased

Déplacé vers le bas [20]: <#>POC concentration

Déplacé vers le bas [21]: <#> Porewaters from the 2016

Supprimé: <#> $\delta^{13}\text{C}_{\text{POC}}$ increased downward from ~ -27 (...)

Supprimé: was also well defined

Supprimé: evolving

Supprimé:) and

Supprimé: decreased

747 between 0.58 and 0.64 psu). Chlorophyll a (Chl a) averaged 3.1 µg/L, and showed a profile with at least three
748 distinctive peaks, (i) between 6 and 9.5 m, (ii) around 12.5 m and (iii) between 16 and 19 m, all reaching ~4 µg/L.
749 The turbidity profile showed a pronounced increase from 16 to 19 m. The pH profile showed important variation,
750 from 9.15 at the lake surface to 8.75 between 6.5 and 10 m, further decreasing to 7.5 between 16 and 26 m. Based
751 on the temperature profiles, epi-, meta- and hypolimnion layers of Lake La Alberca de los Espinos in May 2019
752 broadly extended from 0-5, 5-12 and 12-30 m, respectively (Fig. 2). The conductivity and pH profiles, however,
753 show that different conditions prevail at the top and bottom of the hypolimnion.

754 Dissolved inorganic carbon (DIC) concentration progressively increased from 6.8 mM at 5 m to 8.7 mM at 26 m.
755 The pCO₂ calculated for surface waters was near equilibrium with atmospheric pCO_{2atm}, but strongly increased
756 with depth, up to ~ 40 times the pCO_{2atm} (Table S2). The δ¹³C_{DIC} first decreased from about -2.5 ‰ to -4.1 ‰
757 between 5 and 10 m, before increasing again up to -2 ‰ at 25 m. Particulate organic carbon (POC) concentrations
758 reached minimum values of 0.02 mM at 10 m but rose to maximum values in the hypolimnion (0.06 mM). The
759 C:N molar ratio of particulate organic matter (POM) progressively decreased from 8.5 at the surface to less than
760 6.5 in the hypolimnion. The δ¹³C_{POC} had minimum values at 10 and 17 m (-28.3 and -29 ‰, respectively). Above
761 and below these depths, δ¹³C_{POC} averaged -26.4 ± 0.5 ‰.

762 Dissolved sulfates as measured by chromatography were only detectable at 5 m with a low concentration of 12 µM,
763 while total dissolved S measured by ICP-AES, showed values in the hypolimnion higher than in the upper layers
764 (~ 10.3 vs. 7.4 µM, Table S4). Dissolved Mn concentrations decreased from 1.5 to 0.5 µM between 5 and 10 m,
765 then increased to 2 µM at 25 m. Aqueous Fe was only detectable at 25 m with a concentration of 0.23 µM
766 (Table S4). In parallel, particulate S concentrations increased with depth, with a marked increase from 0.1 to
767 0.6 µM between 20 and 25m. This was spatially correlated with a 25-fold increase in particulate Fe (from 0.2 to
768 5.97 µM). Particulate Mn showed a peak between 17 and 20 m around 1 µM, contrasting with values lower than
769 0.15 µM in the rest of the water column (Fig. 2, Table S5).

770 In the first centimeters of sediments, DIC concentration in the porewater varied between ~ 11 and 12 mM and
771 δ¹³C_{DIC} varied between +8 and +10 ‰ (Figs. 3, 4). Surficial sedimentary carbonates corresponded to calcite and
772 had a δ¹³C around -1.5 ‰. Sedimentary organic matter had a δ¹³C_{SOC} increasing from ~ -29.4 to -25.5 ‰ and a
773 C:N molar ratio varying between 11.6 and 14.3 (Figs. 3, 4; Table S3).

774 4.2. Lake La Preciosa

776 Lake La Preciosa was also stratified at the time of sample collection (Fig. 2). Temperature decreased from ~ 20 °C
777 at the surface to 16 °C at 15m depth. Conductivity showed the same trend with values between 2.24 and
778 2.22 mS/cm (salinity around 1.15 psu). Dissolved O₂ was oversaturated at the lake surface (120 %, i.e., 8.4 mg/L),
779 rapidly decreasing to 0 between ~ 8 and 14 m, while the ORP decreased right below 16 m. Chl a concentration
780 averaged 3 µg/L, and recorded the highest peak compared to the other lakes (about 9 µg/L at 10 m) before
781 decreasing to 0.7 µg/L below 15 m. Turbidity showed a large peak between 16 and 19 m. The pH showed a small
782 decrease from 9 to 8.8 between the surface and 15 m depth. Based on the temperature profiles, epi-, meta- and
783 hypolimnion layers of La Preciosa in May 2019 broadly extended from 0-6, 6-15 and 15-46 m, respectively
784 (Fig. 2).

- Supprimé: La Alberca had relatively high chlorophyll a [...]
- Supprimé: on average) but
- Supprimé: all reaching approximately 4 µg/L. They were [...]
- Supprimé: at
- Supprimé: .
- Supprimé: relatively
- Supprimé: variations
- Supprimé: can be defined as extending
- Supprimé:
- Supprimé: Though we notice *via* the
- Supprimé: The
- Supprimé: Calculated
- Supprimé: at the
- Supprimé: were
- Supprimé: S1
- Supprimé: at
- Supprimé: and then increased back,
- Supprimé: increased back
- Supprimé: (~
- Supprimé: 05
- Supprimé: below
- Supprimé:
- Supprimé: was around
- Mis en forme [...]
- Supprimé: S2
- Supprimé: S2
- Supprimé: S3
- Supprimé: the
- Supprimé: porewater
- Supprimé: and
- Supprimé: ~ 11 and 12 mM and between
- Supprimé: ‰, respectively
- Supprimé: globally
- Supprimé: 3
- Mis en forme [...]
- Supprimé: Lake [...]
- Mis en forme [...]
- Déplacé (insertion) [15]
- Mis en forme [...]
- Déplacé (insertion) [16]
- Mis en forme [...]
- Déplacé (insertion) [17]
- Déplacé (insertion) [18]

823 The DIC concentration was constant throughout the water column at 13.3 mM, with an exception at 12.5 m, where
 824 it decreased to 11.5 mM (Fig. 3, Table S1). Calculated pCO_2 at the surface represented about two times the
 825 atmospheric pCO_{2atm} (Table S2). The $\delta^{13}C_{DIC}$ decreased from about 0.5 ‰ to -0.36 ‰ between the surface and the
 826 hypolimnion. The POC concentration decreased from ~0.06 mM in the epi-/metalimnion to 0.02 mM in the
 827 hypolimnion. Similarly, $(C:N)_{POM}$ decreased from ~11.2 in the epi-/metalimnion to 7.6 in the hypolimnion. The
 828 $\delta^{13}C_{POC}$ increased downward from ~ -27 to -25 ‰ with a peak to -23.5 ‰ at 15 m.
 829 In the first 10 cm of sediments, $\delta^{13}C_{SOC}$ values increased downwards from ~ -25.5 to -23.2 ‰ and C:N molar ratio
 830 from 9.8 to 11 (Figs. 3, 4; Table S3). Carbonates corresponded to aragonite and calcite and had a bulk C isotope
 831 composition averaging 2.6 ‰ (Table S3). Porewaters from the 2016 La Preciosa core were not retrieved.

Déplacé (insertion) [19]

Déplacé (insertion) [20]

Déplacé (insertion) [21]

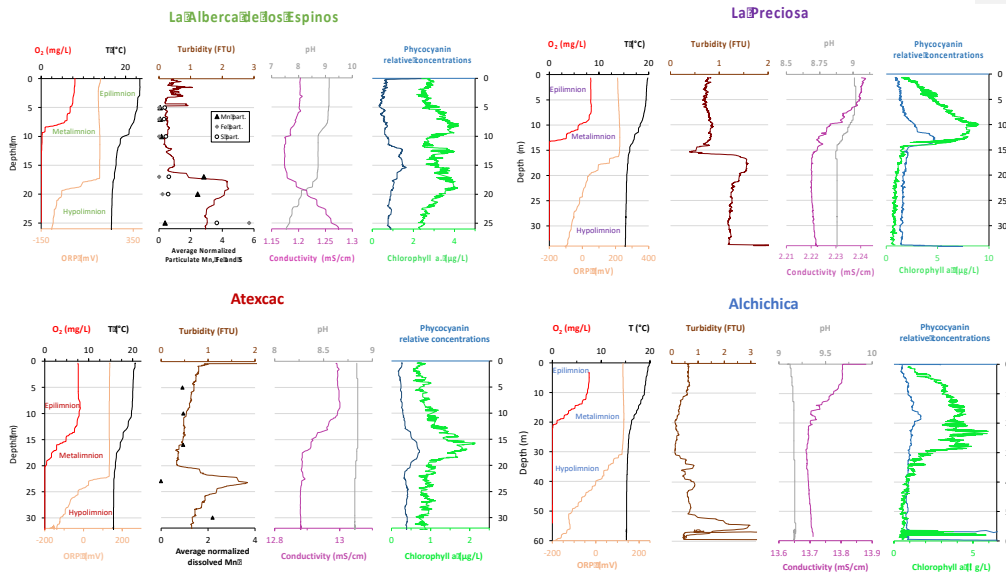


Figure 2. Physico-chemical parameters depth profiles in La Alberca de los Espinos, La Preciosa, Atexcac and Alchichica in May 2019 including: dissolved oxygen concentration (mg/L), water temperature (°C), oxidation-reduction potential (ORP, mV), turbidity (Formazin Turbidity Unit), pH, conductivity (mS/cm), phycocyanin and chlorophyll a pigments (µg/L). Absolute values for phycocyanin concentrations were not determined; only relative variations are represented (with increasing concentrations to the right). Discrete concentration values of dissolved Mn in Atexcac and particulate Mn, Fe and S in La Alberca, normalized by their respective average are represented. Epi-, meta- and hypo-limnion layers are depicted for each lake according to temperature profiles. The three layers closely corresponded to oxygen-rich, oxygen-poor and intermediate zones (except in La Preciosa where the oxycline was slightly thinner than the thermocline layer, ~5 vs. 8 m).

832

833 4.3. Lake Atexcac

Déplacé (insertion) [12]

834 Stratification of the Lake Atexcac water column was also very well defined (Fig. 2). Temperature decreased from
 835 ~ 20.6 °C at the surface to reach 16 °C below 20 m. Conductivity showed the same trend with values between 13
 836 and 12.8 mS/cm near the surface (salinity around 7.4 psu). Dissolved O_2 was slightly oversaturated at the lake

837 surface (115 % or 7.6 mg/L), rapidly decreasing to 0 mg/L between ~ 10 and 20 m, while ORP signal decreased
838 below a depth of 22 m. Chl a averaged 1 µg/L and showed a narrow peak centered at around 16 m, reaching
839 ~2 µg/L. Turbidity showed a pronounced increase below 20 m, peaking at 23.3 m and returning to surface values
840 at 26 m. The pH remained around 8.85 throughout the water column. Based on the temperature profiles, the epi-,
841 meta- and hypolimnion of Atexcac in May 2019 broadly extended from 0-10, 10-20 and 20-39 m, respectively
842 (Fig. 2).

Déplacé (insertion) [13]

843 The DIC concentration was around 26 mM throughout the water column, except at 23 m where it decreased to
844 24.2 mM (Fig. 3, Table S1). Calculated pCO₂ was about five times higher than the atmospheric pCO_{2,atm}
845 (Table S2). The δ¹³C_{DIC} was stable around 0.4 ‰ in the epi-/metalimnion, but increased to 0.9 ‰ at 23 m and
846 reached 0.2 ‰ minimum values at the bottom of the lake. The POC concentration was ~ 0.05 mM in the epi-
847 /metalimnion, decreasing to 0.02 mM in the hypolimnion. The C:N molar ratio of POM showed the same depth
848 profile, decreasing from ~9.6 in the epi-/metalimnion to 6.6 in the hypolimnion (Fig. 3). The δ¹³C_{POC} showed
849 minimum values in the epi-/metalimnion (-29.3 ‰ at 16 m) and increased to -26.5 ‰ in the hypolimnion.

Déplacé (insertion) [14]

850 Dissolved sulfate concentration was relatively stable at ~ 2.51 mM throughout the water column but increased to
851 2.64 mM at 23 m. Dissolved Mn concentration was constant at 1 µM down to 16 m before dropping to 0 at 23 m,
852 and increasing again to 2.35 µM at 30 m (Fig. 2; Table S4). Similar depth profiles were found for other heavy
853 elements as well, including Cu, Sr, Ba or Pb among others.

854 In the first 12 cm of sediments, DIC concentration in the porewater varied between ~ 21 and 26 mM, and δ¹³C_{DIC}
855 was around 0 ‰. Carbonates corresponded to aragonite and calcite and had a bulk C isotope composition between
856 2.1 and 2.6 ‰ (Table S3). Sedimentary organic matter had a δ¹³C_{SOC} averaging -26.8 ± 0.1 ‰ and a C:N molar
857 ratio increasing from 8 to 10 (Figs. 3, 4; Table S3).

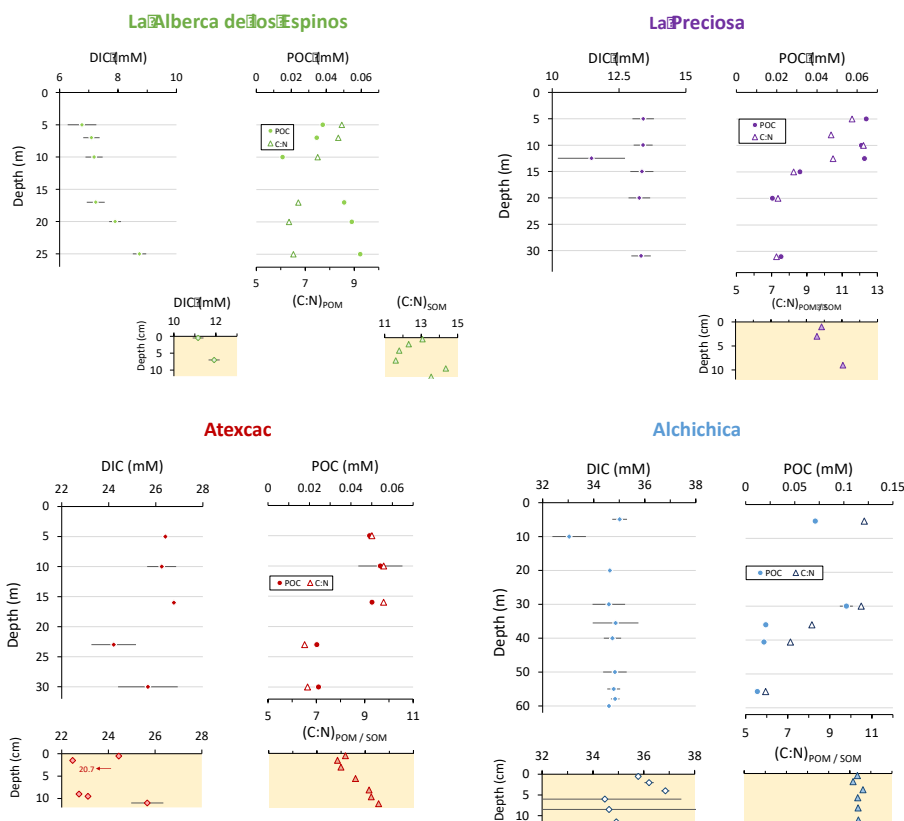


Figure 3. Concentrations in mmol/L (mM) of DIC, DOC, POC and sum of all three reservoirs, C:N molar ratios of POM as a function of depth in the water columns, as well as DIC concentrations in the surficial sediment porewaters and C:N molar ratios of sedimentary OM. Porewaters from La Preciosa's 2016 core were not retrieved.

858

859 4.4. Lake Alchichica

860 The water column of Lake Alchichica showed a pronounced stratification compared to previous years at the same
 861 period (Fig. 2, Fig. S2; Lugo et al., 2000; Adame et al., 2008; Macek et al., 2020). Temperature decreased from
 862 ~ 20 °C at the surface to 15.5 °C at depths below 30 m. Conductivity showed the same trend with values between
 863 around 13.8 mS/cm (salinity decreasing from 7.9 to 7.8 psu). Dissolved O₂ was slightly oversaturated at the lake
 864 surface (112 % or 7.5 mg/L), rapidly decreasing to 0 mg/L between ~ 10 and 20 m. The ORP followed a similar
 865 trend but decreasing below 30 m only. The offset between O₂ exhaustion and decrease of the ORP can be explained
 866 by the presence of other oxidant species and/or extended Chl a peaks (supplementary text 1). Chl a averaged
 867 2 µg/L, with a broad peak extending from ~ 7 to 29 m (averaging 4 µg/L and showing a narrow 6 µg/L maximum
 868 values at 23 m. Then, it decreased to minimum values of ~ 0.5 µg/L in the lower water column. The pH remained

Déplacé (insertion) [9]

Déplacé (insertion) [10]

869 constant at -9.2 over the whole water column. Based on the temperature profiles, the epi-, meta- and hypolimnion
 870 layers of Lake Alchichica in May 2019 extended from 0-10, 10-20 and 20-63 m, respectively (Fig. 2).

871 The DIC concentration was around 34.8 mM throughout the water column, except at 10 m where it decreased to
 872 33 mM (Fig. 3; Table S1). Calculated pCO_2 was about three times higher than the atmospheric pCO_{2atm} (Table S2).
 873 The $\delta^{13}C_{DIC}$ decreased from 2 to ~ 1.5 ‰ between 5 and 60 m depth (Fig. 4; Table S1). The POC concentration
 874 was ~ 0.09 mM in the epi-/metalimnion, decreasing to 0.02 mM in the hypolimnion. The $\delta^{13}C_{POC}$ increased from
 875 -26.5 ‰ in the top 30 m to -24.1 ‰ at 55 m. The C:N molar ratio of POM showed a similar profile with values
 876 around 10.5 down to 30 m, progressively decreasing towards 5.9 at 55 m (Fig. 3; Table S1).

877 In the first 12 cm of sediments, porewater DIC had a concentration of ~ 35.5 mM and $\delta^{13}C_{DIC}$ decreased from 0.4
 878 to -0.5 ‰. Solid carbonates were contained within several phases (aragonite, hydromagnesite, huntite and calcite)
 879 and had a bulk C isotope composition around 4.6 ‰ (Table S3). Sedimentary organic matter had a $\delta^{13}C_{SOC}$
 880 increasing from -25.7 to -24.5 ‰ and a constant C:N molar ratio slightly higher than 10 (Figs. 3, 4; Table S3).

881

Déplacé (insertion) [11]

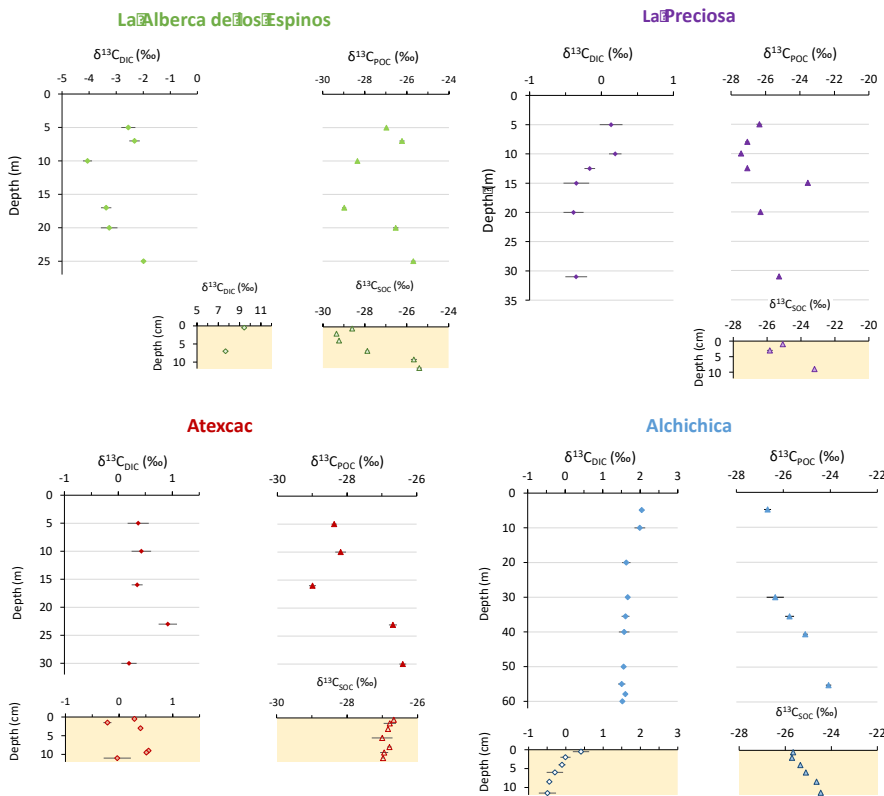


Figure 4. Isotopic compositions of DIC and POC reservoirs as a function of depth in the water columns, as well as isotopic compositions of the porewater-DIC and total organic carbon from the surficial sediments.

5. DISCUSSION

5.1. Inorganic Carbon: origins and implications of the alkalinity/DIC gradient

5.1.1 Sources of DIC and origin of the inter-lake alkalinity gradient

Salinity and DIC concentration gradually increase from La Alberca de los Espinos (0.6 psu, 7 mM) to Alchichica (7.9 psu, 35 mM), while La Preciosa (1.15 psu, 13 mM) and Atexcac (7.44 psu, 26 mM) have intermediate values (Table 1 and S1). This trend matches the alkalinity gradient (with values of ~ 8, 15, 32 and 47 meq/L, Fig. S3a) previously described for these lakes (Zeyen et al., 2021), consistent with the fact that alkalinity is mainly composed of HCO_3^- and CO_3^{2-} ions in most natural waters. This alkalinity gradient may result from different concentration stages of an initial dilute alkaline water (Zeyen et al., 2021), ultimately controlled by differences in hydrological regime between the four lakes. In the SOB, the weathering of basaltic/andesitic bedrock (Armienta et al., 2008; Carrasco-Núñez et al., 2007; Lelli et al., 2021) and Cretaceous limestone (with $\delta^{13}\text{C} \approx 0 \pm 1 \text{‰}$; Gonzales-Partida et al., 1993; Armstrong-Altrin et al., 2011) favors the inflow of more alkaline and DIC-concentrated groundwater than in La Alberca, which lies on an essentially basaltic basement (Rendon-Lopez, 2008; Siebe et al., 2014; Zeyen et al., 2021). The SOB is currently experiencing higher rates of evaporation than precipitation (Alcocer, 2021), which may play an important role in concentrating solutes and decreasing the water level in La Preciosa, Atexcac, and Alchichica (Anderson and Stedmon, 2007; Zeyen et al., 2021). Substantial "sub-fossil" microbialite deposits emerge well above the current water level in lakes Atexcac and Alchichica, confirming this fall in water level (~15 m for Atexcac, and ~5 m for Alchichica). Scattered patches of microbialites emerge at La Preciosa (suggesting a water level decrease of ~6 m). By contrast, emerged microbialites are virtually absent in Lake La Alberca de los Espinos (Fig. S1).

Additional local parameters, such as variable groundwater paths and fluxes (Furian et al., 2013; Mercedes-Martín et al., 2019; Milesi et al., 2020; Zeyen et al., 2021), most likely play a role in explaining some of the variation in DIC concentration between lakes. La Preciosa's water composition significantly differs from that of Atexcac, and Alchichica, despite a similar geological context and climate (all are located within 50 km², Fig. 1). Groundwater in the SOB area becomes more saline as it flows towards the center of the basin and through the crater lakes (Silva Aguilera, 2019; Alcocer, 2021). Since groundwater flows through La Preciosa first, it becomes more concentrated as it enters Alchichica (Silva Aguilera, 2019; Alcocer, 2021; Lelli et al., 2021). Different regimes of volcanic CO₂ degassing into these crater lakes may also contribute to variation in the C mass balance and $\delta^{13}\text{C}_{\text{DIC}}$ values between the four lakes. Near the lakes from the SOB area, geothermal fluids derived from meteoric waters have been shown to interact with deep volcanic fluids as well as the calcareous basement rocks (Peiffer et al., 2018; Lelli et al., 2021). In the water column of La Alberca, $\delta^{13}\text{C}_{\text{total}}$ averages -4.8 ‰ (Havas et al., submitted). This isotopic composition is very similar to signatures of mantle-CO₂ (Javoy et al., 1986; Mason et al., 2017), which could buffer the overall C isotope composition of this lake. La Alberca is located on top of a likely active normal fault (Siebe et al., 2012), favoring the ascent of volcanic gases.

Differences in the remineralization rate of organic carbon (OC) could also contribute to the heterogeneous DIC content among the lakes. However, assuming that all OC from the lakes ultimately remineralized into DIC, it would still represent only a small proportion of the total carbon (9 ‰ for La Alberca, ~5 ‰ for La Preciosa and Alchichica, and 16 ‰ for Atexcac, Havas et al., submitted). From an isotopic mass balance perspective, Lake La

Supprimé: Table 2. Concentrations and isotopic compositions of dissolved inorganic carbon (DIC) and particulate organic carbon (POC) and C:N molar ratios of particulate organic matter (POM). ¶

Mis en forme : Numéros + Niveau : 1 + Style de numérotation : 1, 2, 3, ... + Commencer à : 1 + Alignement : Gauche + Alignement : 0.63 cm + Retrait : 1.27 cm

Supprimé: inter-lake

Supprimé: Salinity and DIC gradually increase from Lake La Alberca de los Espinos (~0.6 psu and 7 mM) to Alchichica (~7.9 psu and 35 mM), while lakes La Preciosa and Atexcac have intermediate values of 1.15 and 7.44 psu and 13 and 26 mM, respectively (Table 1 and 2). This matches a gradient of alkalinity (with values of ~ 8, 15, 32 and 47 meq/L, Fig. S3a) previously described for these lakes (Zeyen et al., 2021), consistently with the fact that alkalinity is mostly composed of HCO_3^- and CO_3^{2-} ions in most natural waters. This alkalinity gradient may result from different concentration stages of an initial dilute alkaline water (Zeyen et al., 2021), those different concentration stages being ultimately controlled by the different hydrological regimes of the lakes. First, the weathering of Cretaceous limestone in the SOB (with a $\delta^{13}\text{C}$ of approximately $0 \pm 1 \text{‰}$; Gonzales-Partida et al., 1993; Armstrong-Altrin et al., 2011) together with basaltic/andesitic bedrock (Armienta et al., 2008; Carrasco-Núñez et al., 2007; Lelli et al., 2021) favors the inflow of more alkaline and DIC-concentrated groundwaters than in Lake La Alberca which lies on an essentially basaltic basement (Rendon-Lopez, 2008; Siebe et al., 2014; Zeyen et al., 2021). {"citationID": "wxjCvLQB", "properties": {"formattedCitation": "(Rendon-Lopez, 2008; Siebe et al., 2014; Zeyen et al., 2021)", "plainCitation": "(Rendon-Lopez, 2008; Siebe et al., 2014; Zeyen et al., 2021)", "noteIndex": 0}, "citationItems": [{"id": 427, "uris": ["http://zotero.org/users/6690596/items/HSE8CNXR"], "uri": "http://zotero.org/users/6690596/items/HSE8CNXR"}, {"id": 427, "type": "article", "title": "Limnología física del lago crater los Espinos, Municipio de Jiménez Michoacán", "URL": "https://www.google.com/url?sa=t&rcet=j&q=&esrc=s&source=web&cd=&ved=2ahUKEwjxIYXR26z2AhVPzRoKHbDrCQ0QFnoECAUQAQ&url=http%3A%2F%2Fbibliotecavirtual.dgb.umich.mx%3A8083%2Fxmlui%2Fhandle%2FDGB_UMICH%2F5774&usg=AOvVaw35MpX..."}]

Supprimé: ...such as variablevarying...groundwater paths and fluxes (Furian et al., 2013; Mercedes-Martín et al., 2019; Milesi et al., 2020; Zeyen et al., 2021),...most likely play a role in explaining somepart...of the variationvariations...in DIC concentration between lakes. For example, Lake ...a (...)

Mis en forme : Couleur de police : Texte 1

Supprimé: may partially explain the striking increases of P_{CO2} and [DIC] and decrease of pH observed at depth (Table S1; Figs. 2 and 3). Moreover, this lake

Mis en forme

Supprimé: , which is favorable to

Mis en forme : Couleur de police : Texte 1

Supprimé: Last, different ...emineralization rates...of organic carbon (OC) could also contribute tobe a source of heterogeneity between...the heterogeneous DIC content amongcontents of...the lakes. However, assuming that all organic carbon (...C)...from the lakes ultimately

1237 Alberca exhibits more negative $\delta^{13}\text{C}_{\text{DIC}}$ (and $\delta^{13}\text{C}_{\text{carb}}$), slightly closer to OC signatures, whereas the $\delta^{13}\text{C}_{\text{DIC}}$ of the
1238 three SOB lakes lie very far from OC isotopic signatures (Fig. 4). Dense vegetation surrounds La Alberca (Fig. S1),
1239 making it the only lake in this study where OC respiration could be a significant source of inorganic C to the water
1240 column (potentially influencing the P_{CO_2} , [DIC] and pH profiles described above).

Supprimé: 4). This latter lake also stands out from the others because of the dense

Supprimé: surrounding it

Supprimé:

Supprimé:). Therefore, La Alberca seems to be

Déplacé (insertion) [22]

Mis en forme : Police :Non Gras, Non Italique

Mis en forme : Aucun(e)

1241
1242
1243 In summary, a combination of very local and external environmental factors generates the contrasting water chemistries of the lakes, notably a gradient in their alkalinity/[DIC]. This variability stems from the exact nature of the basement rocks, the distinct groundwater flow paths feeding the lakes, differences in evaporation rates, and potentially different volcanic- CO_2 degassing regimes.

1243 5.1.2 Influence of alkalinity on physico-chemical stratification in the four lakes

1244 Stratified water columns can sustain strong physico-chemical gradients, where a wide range of biogeochemical reactions impacting the C cycle can take place (e.g. Jézéquel et al., 2016). In the four lakes studied here, the evolution of pH with depth exemplifies the interplay between the alkalinity gradient, the physico-chemical stratification of the lakes, and their respective C cycle. The pH shows a stratified profile in La Alberca and La
1245 Preciosa, but remains constant in Atexcac and Alchichica. The decline in pH at the oxycline of La Preciosa is associated with the decrease in POC and chlorophyll a concentrations and $\delta^{13}\text{C}_{\text{DIC}}$ values, reflecting the impact of oxygen respiration (i.e. carbon remineralization) at this depth (Figs. 2-4). In La Alberca, the surface waters are
1246 markedly more alkaline than the bottom waters, with a two-step decrease in pH occurring at 8 m and 17 m (with a total drop of 1.5 pH unit). As in La Preciosa, this likely results from high OM respiration, although input of volcanic acidic gases (e.g. dissolved CO_2 with $\delta^{13}\text{C} \sim -5\text{‰}$) might also contribute to the pH decrease in the bottom waters, reflected by negative $\delta^{13}\text{C}_{\text{DIC}}$ signatures and an increase of [DIC] and conductivity in the hypolimnion (Figs. 2 and
1247 4). By contrast, while the same evidence for oxygen respiration ([POC], chlorophyll a) can be detected in the other two lakes, it does not impact their pH profile in a similar way (Fig. 2). This result suggests that the acidity generated by these reactions is buffered by the much higher alkalinity measured in these two lakes.

Déplacé (insertion) [23]

Mis en forme : Police :Non Italique

Déplacé (insertion) [24]

Mis en forme : Police :Non Italique

1258 is particularly important considering the critical interplay between pH and biogeochemical reactions affecting the C cycle (e.g. Soetaert et al., 2007).

Déplacé (insertion) [25]

Mis en forme : Police :Non Italique

1259 External forcings such as lake hydrology and fluid sources thus impact the alkalinity buffering capacity of these lakes and influence the vertical pH profile of the water columns. This

Mis en forme : Police :Gras

1261 5.1.3 Sinks of DIC along the alkalinity gradient

1262 Interplay between pH and sources of alkalinity/DIC in the lakes also has a strong impact on their C storage capacity as it can result in different fluxes of the C sinks (inorganic and organic C precipitation / sedimentation, CO_2 degassing).

Déplacé (insertion) [26]

Mis en forme : Numéros + Niveau : 1 + Style de numérotation : 1, 2, 3, ... + Commencer à : 1 + Alignement : Gauche + Alignement : 0.63 cm + Retrait : 1.27 cm

1265 Alkaline pH can store large quantities of DIC because it favors the presence of HCO_3^- and CO_3^{2-} species over H_2CO_3^* (the intermediate species between gaseous $\text{CO}_2(\text{g})$ and bi-/carbonate ions, defined here as the sum of H_2CO_3 and $\text{CO}_2(\text{aq})$). Carbonate and bicarbonate ions represent over 99% of total DIC in the four lakes (Table S2). In La
1266 Alberca de los Espinos, the lake with the lowest DIC, the surface water pCO_2 is slightly lower than atmospheric $\text{pCO}_{2\text{atm}}$ (Table S2). By contrast, large amounts of CO_2 degas at the surface of the SOB lakes, as indicated by their

1275 elevated surface water $p\text{CO}_2$, from 2 to 5 times higher than atmospheric $p\text{CO}_{2\text{atm}}$ (Table S2). These observations
1276 are consistent with the notion that higher DIC concentrations favor CO_2 degassing through higher $p\text{CO}_2$ (e.g.
1277 Duarte et al., 2008). Although La Alberca and Alchichica (the two endmembers of the alkalinity gradient) have
1278 the same surface water pH, CO_2 degassing is three times higher at Alchichica, for a given value of gas transfer
1279 velocity.

1280 amounts of carbonate deposits (Zeyen et al., 2021). The occurrence of microbialites increases along the alkalinity
1281 gradient, with limited presence at La Alberca, and more massive deposits at Atexcac and Alchichica (Zeyen et al.,

Déplacé (insertion) [27]

Another important C sink for these lakes is the precipitation of carbonate minerals, found in the microbialites
and lake sediments. Lake alkalinity and resulting mineral saturation index greatly influence the amount of C
precipitated from the lake waters. Although the four lakes are supersaturated with aragonite, calcite and the
precursor phase monohydrocalcite, they present highly contrasted

1282 2021; Fig. S1). Similarly, surficial sediments contain only 16 wt. % for La Alberca, but from 40 to 62 wt. %
1283 carbonates for the SOB lakes (Table S3). Thus, the SOB lakes seem to bury more C than La Alberca de los Espinos.

Déplacé (insertion) [28]

1284 Nonetheless, the data from May 2019 indicate that La Alberca was the only one of the four lakes with a $p\text{CO}_2$
1285 slightly lower than atmospheric $p\text{CO}_{2\text{atm}}$, thus representing a net sink of C. Classifying the three other lakes as net

Déplacé (insertion) [29]

1286 C sources or sinks – notably in order to see the influence of their respective position in the alkalinity gradient –
1287 will require a more detailed description of C in- and out-fluxes since they all store and emit significant amounts
1288 of C (as organic and inorganic C deposits and via CO_2 degassing, respectively). However, this is out of the scope
1289 of the present study.

Mis en forme : Police :Gras

1290

1291 **5.1.4 Isotopic signatures of inorganic C in the four lakes ($\delta^{13}\text{C}_{\text{DIC}}$ and $\delta^{13}\text{C}_{\text{Carbonates}}$)**

1292 $\delta^{13}\text{C}_{\text{DIC}}$ in La Alberca is consistent with influence of remineralized OC and/or volcanic CO_2 . The $\delta^{13}\text{C}_{\text{DIC}}$ in the
1293 SOB lakes suggests groundwater $\delta^{13}\text{C}_{\text{DIC}}$ values resulting from the dissolution of the Cretaceous limestone

Déplacé (insertion) [30]

The DIC isotopic composition of the lakes (between ~ -3 and $+2$ ‰ on average; Table S1) is consistent with the
DIC sources described above. The lower
1294 basement.

1295 for lakes with a pH around 9 (Bade et al., 2004), where DIC is dominated by HCO_3^- . However, the pH values of
1296 the four lakes studied here are too similar to explain the significant difference between their $\delta^{13}\text{C}_{\text{DIC}}$ (Fig. 4;

Déplacé (insertion) [31]

By controlling DIC speciation ($\text{H}_2\text{CO}_3/\text{CO}_{2(\text{aq})}$, HCO_3^- , CO_3^{2-}), pH also strongly influences $\delta^{13}\text{C}_{\text{DIC}}$. Indeed, there
is a temperature-dependent fractionation of up to 10 ‰ between the different DIC species (Emrich et al., 1970;
Mook et al., 1974; Bade et al., 2004; Table S6). The Mexican lakes present $\delta^{13}\text{C}_{\text{DIC}}$ values that are common
1297 $p=4.2 \times 10^{-3}$ for La Preciosa and Atexcac, which have the closest $\delta^{13}\text{C}_{\text{DIC}}$). Part of the variability of $\delta^{13}\text{C}_{\text{DIC}}$ among

1298 the lakes may result from their distinct evaporation stages, as the mean $\delta^{13}\text{C}_{\text{DIC}}$ values of the lakes broadly correlate
1299 with their salinity/alkalinity (Fig. S3b). Evaporation generally increases the $\delta^{13}\text{C}_{\text{DIC}}$ of residual waters by

1300 increasing lake $p\text{CO}_2$ and primary productivity. This bolsters CO_2 degassing and organic C burial, which have low
1301 $\delta^{13}\text{C}$ compared to DIC (e.g., Li and Ku, 1997; Talbot, 1990). Accordingly, the $p\text{CO}_2$ of La Alberca is lower than

Déplacé (insertion) [32]

1302 that of the other lakes (Table S2). The $\delta^{13}\text{C}_{\text{DIC}}$ in lakes with lower DIC concentrations is expected to be more easily
1303 influenced by exchanges with other carbon reservoirs, such as organic carbon (through photosynthesis/respiration),

1304 or other DIC sources (e.g., depleted volcanic CO_2 or groundwater DIC), compared with buffered, high DIC lakes
1305 (Li and Ku, 1997). As a result, the low DIC/alkalinity concentration in La Alberca features the lowest $\delta^{13}\text{C}_{\text{DIC}}$ of

Déplacé (insertion) [33]

1306 the four lakes, likely reflecting organic and/or volcanic C influence and thus higher responsiveness to
 1307 biogeochemical processes of the inorganic C reservoir. By contrast, the three SOB lakes exhibit $\delta^{13}\text{C}_{\text{DIC}}$ with less
 1308 internal variability, with a maximum amplitude of 0.7 ‰ within a single water column.

1309 $\delta^{13}\text{C}_{\text{Carb}}$ also follows and reflects the alkalinity gradient, with the lowest $\delta^{13}\text{C}_{\text{Carb}}$ found in the surficial sediments
 1310 of La Alberca (~ -1.5 ‰), intermediate values in La Preciosa and Atexcac (~-2.5 ‰), and the highest values in

Surficial sedimentary carbonates are in isotopic equilibrium with the $\delta^{13}\text{C}_{\text{DIC}}$ of the water columns, within the
 uncertainty of $\delta^{13}\text{C}_{\text{DIC}}$ measurement, and more specifically with the $\delta^{13}\text{C}_{\text{DIC}}$ values at the oxycline/thermocline of
 the lakes (Tables S6 and S7). This is estimated by correcting the carbonates C isotope composition ($\delta^{13}\text{C}_{\text{Carb}}$) by
 the fractionation value between DIC and the different carbonate mineralogies (supplementary text S2).
 Therefore, the

1311 Alchichica (~ +4.6 ‰) (Table S3).

1312
 1313 In summary, although all four lakes present the same general structure and environmental conditions (i.e. tropical
 1314 alkaline stratified crater lakes), external and local factors (e.g. hydrology, fluid sources, and stratification
 1315 characteristics) result in contrasting water chemistry compositions, which have a critical impact on the physico-
 1316 chemical depth profiles of each lake and their biogeochemical carbon cycle functioning. These external factors
 1317 represent a first-order control on the size, isotopic composition, and responsiveness to biogeochemical processes
 1318 of the inorganic C reservoir. Lakes with the highest alkalinity/DIC content will poorly record internal biological
 1319 processes. Interestingly, C storage in mineral carbonates seems to be significant in watersheds where carbonate
 1320 deposits pre-exist in the geological substratum (here, the Cretaceous limestone basement), providing more alkaline
 1321 and C-rich sources.

Déplacé (insertion) [34]

Mis en forme : Gauche, Interligne : simple,
 Position :Horizontal : 2.17 cm, Par rapport à : Page,
 Vertical : 1.5 cm, Par rapport à : Paragraphe, Horizontal
 : 0.33 cm

Mis en forme : Espace Après : 0 pt, Interligne : simple,
 Position :Horizontal : 2.17 cm, Par rapport à : Page,
 Vertical : 1.5 cm, Par rapport à : Paragraphe, Horizontal
 : 0.33 cm

Supprimé: Sample name

Mis en forme : Police :Times New Roman, 10.5 pt, Gras,
 Couleur de police : Automatique

Déplacé vers le haut [34]: $\delta^{13}\text{C}_{\text{Carb}}$

Supprimé: Depth

Supprimé: SOC

Déplacé vers le bas [35]: $\delta^{13}\text{C}_{\text{SOC}}$

Supprimé: (C:N)_{SOM}

Déplacé vers le haut [30]: $\delta^{13}\text{C}_{\text{DIC}}$

Supprimé: Carb.

Supprimé: Lake

Mis en forme : Police :Times New Roman, 10.5 pt, Gras,
 Couleur de police : Automatique

Supprimé: DIC

Mis en forme : Police :Times New Roman, Gras,
 Couleur de police : Automatique

S y m b o l s	Mathe matic al Expres sion	Signification
δ		
$\frac{1}{3}$		
$\frac{3}{C}$	$\left(\frac{\left(\frac{^{13}\text{C}}{^{12}\text{C}} \right)_{\text{sample}}}{\left(\frac{^{13}\text{C}}{^{12}\text{C}} \right)_{\text{standard}}} - 1 \right) * 1000$	Relative difference in $^{13}\text{C}:^{12}\text{C}$ isotopic ratio between a sample of a given C reservoir and the international standard "Vienna Pee Dee Bee", expressed in permil (‰). $\delta^{13}\text{C}_{\text{total}}$ represents the weighted average of $\delta^{13}\text{C}$ for all DIC and POC.
$\frac{4}{x}$		

$$\delta^{13}C_X = \frac{1000}{\alpha} \left(\frac{\delta^{13}C_Y}{\delta^{13}C_{CO_2}} - 1 \right)$$

Apparent isotopic fractionation between two reservoirs 'X' and 'Y'. Difference between their measured C isotope compositions approximating the fractionation α in ‰.

Calculated as α_{CO_2} is calculated as $\frac{(\delta^{13}C_X + 1000)/(\delta^{13}C_{CO_2} + 1000)}{\delta^{13}C_X}$ where $\delta^{13}C_X$ is measured and $\delta^{13}C_{CO_2}$ is computed based on DIC isotopic composition and speciation (see supplementary text S3).

1332

1333

1334 **Table 2**

1336 Index for mathematical notations used in the text including C isotopic composition of a reservoir X ($\delta^{13}C_X$), isotopic discrimination between the two carbon reservoirs X and Y ($\Delta^{13}C_{X-Y}$). In the main text, we report organic C isotope discrimination versus both bulk DIC ($\Delta^{13}C_{POC-DIC}$) – in a way to facilitate studies intercomparison and because it is the commonly reported raw measured data (Fry, 1996) – and calculated $CO_{2(aq)}$ (ϵ_{POC-CO_2}) in order to discuss the intrinsic isotopic fractionations associated with the lakes metabolic diversity. All C isotope values and fractionations are reported relative to the international standard VPDB (Vienna Pee Dee Belemnite).

1344 **5.2. Particulate organic carbon: from water column primary production to respiration recycling and sedimentary organic matter**

1345

1346

- Mis en forme
- Supprimé: (molar)
- Supprimé: wt. %
- Supprimé: ‰
- Supprimé: mmol/L
- Supprimé: ‰
- Supprimé: wt. %
- Supprimé: ‰
- Mis en forme
- Mis en forme
- Supprimé: cm
- Mis en forme
- Supprimé: Alchichica
- Supprimé: Alchichica
- Mis en forme
- Mis en forme
- Supprimé: 13.1
- Supprimé: 13.3
- Supprimé: -28.6
- Supprimé: 11.2
- Supprimé: 9.4
- Supprimé: 20
- Supprimé: -1.5
- Supprimé: La Alberca de Los Espinos
- Mis en forme
- Supprimé: ALBESP19_C3_1
- Mis en forme
- Supprimé: 0-1
- Mis en forme
- Déplacé vers le haut [29]: Classifying the three other
- Supprimé: ¶
- Supprimé: ¶
- Déplacé vers le haut [22]: ¶
- Mis en forme
- Supprimé: the lakes' alkalinity on their physico-chemi
- Déplacé vers le haut [23]: Stratified water columns can
- Mis en forme
- Supprimé: Here, temperature, conductivity and O₂ profile
- Déplacé vers le haut [24]: POC and chlorophyll a
- Mis en forme
- Supprimé: In Lake La Alberca, the surface waters are
- Déplacé vers le haut [25]: is particularly important
- Mis en forme
- Mis en forme
- Supprimé: Isotopic signatures of inorganic C in the lak
- Déplacé vers le haut [31]: for lakes with a pH around 9
- Supprimé: However, the pH values of the studied Mexica
- Déplacé vers le haut [32]: Li and Ku, 1997; Talbot,
- Supprimé: Accordingly, the pCO₂ of La Alberca is small
- Déplacé vers le haut [33]: compared with buffered, high
- Mis en forme

1863 **5.2.1. Particulate organic C sources**

1864 *Primary productivity by oxygenic photosynthesis in the upper water column*

1865 All four crater lakes are endorheic basins, with no surface water inflow or outflow. The organic carbon sources
1866 are therefore predominantly autochthonous, resulting mainly from planktonic autotrophic C fixation. This is
1867 supported by C:N ratios of POM that ranged from 6 to 12 in the four lakes, close to the phytoplankton Redfield
1868 but far from land plant ratios. Abundant vegetation covers the crater walls of La Alberca and to a lesser extent
1869 those of Atexcac; some plant debris was observed and sampled from the sediment cores of these two lakes. They
1870 have high C:N ratios (between 24 and 68), typical of plant tissues and significantly higher than those of the bulk
1871 organic matter in the surficial sediments (between 8 and 13) and water column (between 6 and 12) (Fig. 3). Thus,
1872 the allochthonous organic carbon in these two lakes does not significantly contribute to their bulk organic signal.

1873 The importance of planktonic autotrophic C fixation as a major source of POC in the four lakes is further supported
1874 by the assessment of the isotopic discrimination between DIC and organic biomass, expressed as $\Delta^{13}\text{C}_{\text{POC-DIC}}$ and
1875 $\epsilon_{\text{POC-CO}_2}$ (Table 2). The $\Delta^{13}\text{C}_{\text{POC-DIC}}$ varies between ~ -29 and -23 ‰ (corresponding to $\epsilon_{\text{POC-CO}_2}$ between ~ -19 and
1876 -13 ‰) throughout the four water columns, within the typical range of planktonic oxygenic phototrophs (Pardue
1877 et al., 1976; Sirevag et al., 1977; Thomas et al., 2019). Yet, these values exhibit variability – both within a single
1878 water column (up to 4.5 ‰) and among the four lakes (up to 6 ‰, Figs. 4 and 5). This variability may reflect
1879 several abiotic and biotic factors.

1880 Notably, lower DIC availability in La Alberca and La Preciosa probably makes the carboxylation step less limiting
1881 during photosynthesis (e.g. O'Leary, 1988; Descolas-Gros and Fontungne, 1990; Fry, 1996), decreasing $|\epsilon_{\text{POC-CO}_2}|$
1882 in these lakes (between 14.5 and 17.7 ‰ at the peak of Chl. a) compared with Atexcac and Alchichica (Fig. 5a;
1883 between 17.5 and 19.2 ‰). Lower $\text{CO}_{2(\text{aq})}$ availability and/or higher reaction rates result in transport-limited rather
1884 than carboxylation-limited fixation, with smaller C isotope fractionation between POC and DIC (Pardue et al.,
1885 1976; Zohary et al., 1994; Fry, 1996; Close and Henderson, 2020). The isotopic fractionation associated with
1886 diffusion is much smaller than with carboxylation, and a higher proportion of the DIC entering the cells is
1887 converted into organic biomass (e.g. Fogel and Cifuentes, 1993). We consistently notice a correlation among the
1888 lakes between $\alpha(\text{CO}_{2(\text{aq})})$ (or [DIC]) and $|\epsilon_{\text{POC-CO}_2}|$ at depths where oxygenic photosynthetic peaks (Fig. 6).
1889 Furthermore, La Alberca and La Preciosa are considered less oligotrophic than the two other lakes (Lugo et al.,
1890 1993; Vilaclara et al., 1993; Havas et al., submitted), with higher chlorophyll a contents and thus smaller $|\epsilon_{\text{POC-CO}_2}|$
1891 (Fig. 5). Higher water temperatures in La Alberca de los Espinos (by ~ 3 °C) could also partly contribute to a
1892 smaller $|\epsilon_{\text{POC-CO}_2}|$ in this lake (Sackett et al., 1965; Pardue et al., 1976; Descolas-Gros and Fontungne, 1990).

Mis en forme : Normal, Retrait : Gauche : 0.38 cm, Première ligne : 0.25 cm, Sans numérotation ni puces

Supprimé: i.e. there is

Supprimé: Therefore, the...organic carbon sources are therefore predominantly autochthonous, mainly ...resulting mainly from planktonic autotrophic C fixation. This is supported by C:N ratios of POM that ranged from 6 to 12 in the four lakes, close to the phytoplankton Redfield but far from land plant ratios. Abundant vegetation covers the crater walls of Lake ...a Alberca and to a lesser extent those of Lake ...a Atexcac; some plant debris was observed and sampled from the sediment cores of these two lakes. They have had ...high C:N ratios (between 24 and 68), typical of plant tissues and significantly higher than those of the bulk organic matter in the surficial sediments (between 8 and 13) and the ...ater column (between 6 and 12) (Fig. 3). Thus, theTherefore, ...allochthonous organic carbon in these two lakes – albeit present –

Mis en forme : Police :Italique

Supprimé: organic C...in the four lakes is further supported by the assessment of the isotopic discrimination between DIC and organic biomass, expressed as $\Delta^{13}\text{C}_{\text{POC-DIC}}$ and $\epsilon_{\text{POC-CO}_2}$ (Table 2.... The $\Delta^{13}\text{C}_{\text{POC-DIC}}$ varies...between ~ -29 and -23 ‰ (corresponding to $\epsilon_{\text{POC-CO}_2}$ between ~ -19 and -13 ‰)%; Table 5)...throughout the four water columns, withinwhich is in ...the typical range of planktonic oxygenic phototrophs (Pardue et al., 1976; Sirevag et al., 1977; Thomas et al., 2019). Yet, ...these values exhibit variability – both within a single water column (up to 4.5 ‰) and amongbetween...the fourdifferent...lakes (up to 6 ‰, Figs. 4 and 5). This variability may reflecttrace

Supprimé: higher...DIC availability in La AlbercaAlchichica... and La PreciosaAtexcac... probably makes the carboxylation step lessmore

Supprimé: increasing... $|\epsilon_{\text{POC-CO}_2}|$ in these lakes (between 14.5...5 and 17.7 19.2 ... at the peak of Chl. a) compared with Atexcac La Preciosa... and AlchichicaAlberca

Mis en forme : Police :Non Italique

Mis en forme : Couleur de police : Automatique

Supprimé: 14...5 and 19.2 ‰). Lower17.7 ‰). Indeed, lower... $\text{CO}_{2(\text{aq})}$ availability and/or higher reaction rates result transport-limited rather than carboxylation-limited fixation, with and thus,...smaller C isotope fractionation between POC and DIC (Pardue et al., 1976; Zohary et al., 1994; Fry, 1996; Close and Henderson, 2020). TheThis is because the...isotopic fractionation associated with diffusion is much smaller than with carboxylation, and because

Mis en forme : Police :Non Italique

Supprimé: Consistently, we...notice a correlation among the lakes between $\alpha(\text{CO}_{2(\text{aq})})$ (or [DIC]) and $|\epsilon_{\text{POC-CO}_2}|$ at depths where oxygenic photosynthetic peaks (Fig. 6). Furthermore, La Alberca and lakes ...a Preciosa and Alberca...are considered less oligotrophic than the two other lakes (Lugo et al., 1993; Vilaclara et al., 1993; Havas et al., submitted), consistently ...ith higher chlorophyll a contents and thus smaller $|\epsilon_{\text{POC-CO}_2}|$ (Fig. 5). HigherLast, higher

1987 Unlike $\delta^{13}\text{C}_{\text{DIC}}$, organic carbon isotope signatures do not evolve linearly with the alkalinity/salinity gradient,
 1988 suggesting other lake- and microbial-specific controls on these signatures. These controls include: diffusive or
 1989 active uptake mechanisms, specific carbon fixation pathways, the fraction of intracellular inorganic carbon
 1990 released out of the cells, cell size and geometry (Werne and Hollander, 2004 and references therein) and
 1991 remineralization efficiency. Moreover, an increasing amount of isotopic data has evidenced a significant variability
 1992 of the isotopic fractionation achieved by different purified RuBisCO enzymes ($\epsilon_{\text{RuBisCO}}$, Iñiguez et al., 2020), and
 1993 even by a single RuBisCO form (Thomas et al., 2019). Thus, caution should be paid to the interpretation of the
 1994 origin of small isotopic variations of the biomass in distinct environmental contexts because RuBisCO alone can
 1995 be an important source of this variability (Thomas et al., 2019).

Supprimé: isotopic

Supprimé: number

Supprimé: <objet>

Supprimé:

Supprimé: <objet>

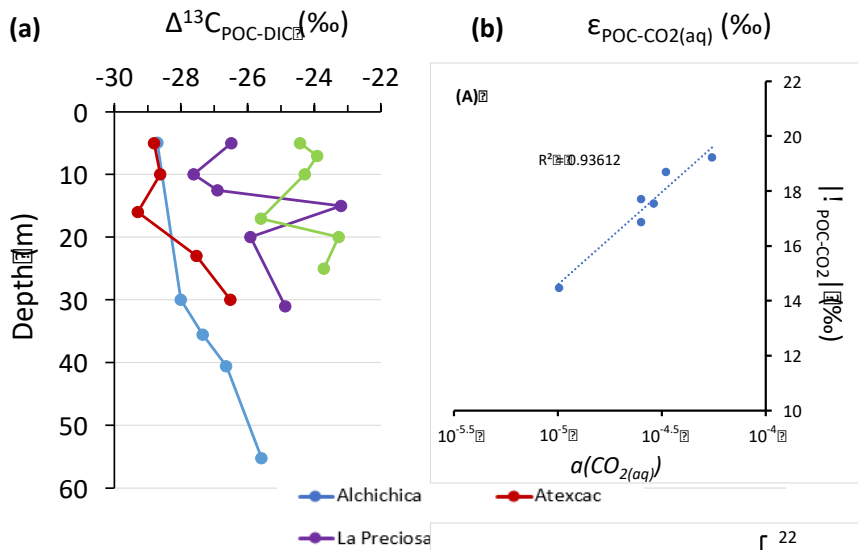
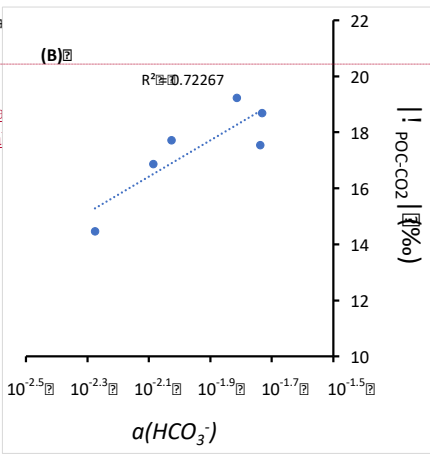


Figure 5. Isotopic fractionations between POC and DIC expressed as a) $\Delta^{13}\text{C}_{\text{POC-DIC}}$ and b) $\epsilon_{\text{POC-CO}_2}$. Refer to Table 1 for details.

Supprimé: Lake

1998 Primary production in the anoxic hypolimnion



2006 Anoxygenic autotrophs commonly thrive in anoxic bottom waters of stratified water bodies (e.g. Pimenov et al.,
 2007 2008; Zyakun et al., 2009; Posth et al., 2017; Fulton et al., 2018; Havig et al., 2018). They have been identified at
 2008 different depths in the four Mexican lakes (Macek et al., 2020; Iniesto et al., 2022). In our samples collected during
 2009 the stratification period, anoxygenic autotrophs appear to have a distinct impact on the C cycle of La Alberca and
 2010 Atexcac only. Lake Atexcac records a concomitant decrease in [DIC] and increase in $\delta^{13}C_{DIC}$ in the anoxic
 2011 hypolimnion at 23 m, below the peak of Chl a, suggesting autotrophic C fixation by chemoautotrophy or
 2012 anoxygenic photosynthesis. The calculated ϵ_{POC-CO_2} at 23 m (-17.3 ‰) is consistent with C isotope fractionation
 2013 by purple- and green-sulfur-anoxygenic bacteria (PSB and GSB), while ϵ_{POC-CO_2} in La Alberca's hypolimnion (~
 2014 -15 ‰) is closer to GSB canonical signatures (Posth et al., 2017 and references therein) (Fig. 5b). In La Alberca,
 2015 anoxygenic primary productivity is suggested by increasing POC concentrations below the oxycline. We also
 2016 observe a Chl a peak in the anoxic hypolimnion of this lake (Fig. 2), which likely represents a bias of the probe
 2017 towards some bacteriochlorophyll pigments typical of GSB (see supplementary text S4). In Atexcac, C fixation by
 2018 anoxygenic autotrophs at 23 m causes a shift in the DIC reservoir, while oxygenic photosynthesis at 16 m does
 2019 not, suggesting that anaerobic autotrophs are the main autotrophic metabolisms in this lake (in terms of DIC
 2020 uptake). In La Alberca, the increase in [POC] to maximum values at depth also supports the predominance of
 2021 anoxygenic *versus* oxygenic autotrophy (Fig. 3). This is similar to other stratified water bodies exhibiting primary
 2022 production clearly dominated by anoxygenic metabolisms (Fulton et al., 2018).

2023 Lastly, at 23 m in Atexcac and 17 m in La Alberca, we find a striking turbidity peak precisely where the redox
 2024 potential and the concentration of dissolved Mn drops (Fig. 2). In Atexcac, the concentration in dissolved metals,
 2025 such as Cu, Pb, or Co also drops at 23 m (Fig. S4). In La Alberca, a peak of particulate Mn concentration is detected
 2026 at 15 m (Fig. 2; data unavailable for Atexcac). This is most likely explained by the precipitation of Mn mineral
 2027 particles, where reduced bottom waters meet oxidative conditions prevailing in the upper waters. These oxidized
 2028 Mn phases can be used as electron acceptors during chemoautotrophy (Havig et al., 2015; Knossow et al., 2015;
 2029 Henkel et al., 2019; van Vliet et al., 2021). Even at a low particle density, such phases can catalyze abiotic oxidation
 2030 of sulfide to sulfur compounds, which in turn can be used and further oxidized to sulfate by phototrophic or
 2031 chemoautotrophic sulfur-oxidizing bacteria (van Vliet et al., 2021). This is also consistent with the small increase
 2032 in [SO₄²⁻] observed at 23 m in Atexcac (Table S4).

2033 In summary, combined POC and DIC data allowed us
 2034 to recognize the most representative autotrophic
 2035 metabolisms in the Mexican lakes. The upper water
 2036 columns are all dominated by oxygenic
 2037 photosynthesis. Lower in the water columns,
 2038 anoxygenic photosynthesis and/or chemoautotrophy
 2039 were found to have a noticeable impact on POC and
 2040 DIC reservoirs in La Alberca and Atexcac only. Their
 2041 activity was associated with metal elements cycling.
 2042 More specifically in La Alberca, the anoxygenic
 2043 phototrophs correspond to GSB.

Figure 6.

Cross plots of DIC species activities *versus* absolute values of calculated C isotopic fractionations between POC and CO₂ at depths of peak oxygenic photosynthesis where data was available (5 and 30 m for Alchichica, 16 m for Atexcac, 10 and 12.5 m for La Preciosa and 7 m for La Alberca). (A) Dissolved CO_{2(aq)} activity and (B) bicarbonate activity as functions of $|\epsilon_{POC-CO_2}|$ in ‰ plus linear correlation trends and corresponding R².

- Mis en forme : Police :Non Italique
- Supprimé: (Pimenov et al., 2008; Zyakun et al., 2009; Posth et al., 2017; Fulton et al., 2018; Havig et al., 2018)
- Supprimé: Consistently, they
- Supprimé: Based on
- Supprimé: results obtained on
- Supprimé: distinctive
- Supprimé: lakes Atexcac and
- Supprimé: Indeed,
- Supprimé: of
- Supprimé: of
- Supprimé: chlorophyll
- Supprimé: isotopes
- Supprimé: moreover
- Supprimé: Besides, we
- Supprimé: .
- Supprimé:
- Supprimé: bacteriochlorophylls
- Supprimé: S3). We notice that in Lake
- Supprimé: at 23 m
- Supprimé: of
- Supprimé: which exhibit
- Supprimé: Last
- Supprimé: Lake
- Supprimé: Lake
- Supprimé:
- Supprimé: Lake
- Supprimé: concentrations of
- Supprimé: metal
- Supprimé: drop
- Supprimé: concentrations
- Supprimé: not available
- Supprimé: as
- Supprimé: Moreover, even
- Supprimé: (van Vliet et al., 2021), which in turn
- Supprimé: . This is also consistent with the small increase of
- Supprimé: S2

2082

2083

5.2.2. Sinks of particulate organic carbon: respiration and sedimentation

2084

Aerobic respiration at the oxycline

2085

At the oxycline of stratified water bodies, aerobic respiration of OM by heterotrophic organisms favors the transition from oxygenated upper layers to anoxic bottom waters. In the water column of the four lakes, $\Delta^{13}\text{C}_{\text{POC-DIC}}$ (and $\epsilon_{\text{POC-CO}_2}$) show increasing values in the hypolimnion, and especially below the chlorophyll a peaks (Figs. 2 and 5). This trend also correlates with increasing $\delta^{13}\text{C}_{\text{POC}}$, decreasing (C:N)_{POM} ratios as well as decreasing POC concentrations except in La Alberca (Figs. 3 and 4). Decreasing POC concentrations near the oxycline and redoxcline are consistent with the fact that part of the upper primary production is degraded deeper in the water columns and/or that there is less primary production in the anoxic bottom waters. Increased $\delta^{13}\text{C}_{\text{POC}}$ in the hypolimnion of the lakes is consistent with heterotrophic activity and points out that POC at these depths could mainly record secondary production rather than being a residue of sinking degraded OM formed by primary production. Heterotrophic bacteria preferentially grow on available ^{13}C -enriched amino acids and sugars, thus becoming more enriched than their C source (Williams and Gordon, 1970; Hayes et al., 1989; Zohary et al., 1994; Briones et al., 1998; Lehmann et al., 2002; Jiao et al., 2010; Close and Henderson, 2020). The decrease in C:N ratios in the POM also reinforces this conclusion since secondary heterotrophic bacteria biomass generally have C:N between 4 and 5 (Lehmann et al., 2002), whereas residual degraded OM from primary producers would carry higher C:N signatures (van Mooy et al., 2002; Buchan et al., 2014). These latter signatures are not recorded by POM in the lower water columns of the lakes (Fig. 3).

2101

The $\delta^{13}\text{C}_{\text{DIC}}$ signatures in La Preciosa and Alchichica are consistent with the mineralization of OM as they exhibit lower values below the oxycline than in surficial waters (Figs. 2 and 4). Similarly to what is observed in several other water bodies and notably stratified water columns such as the Black Sea (e.g. Fry et al., 1991), surface photosynthesis increases $\delta^{13}\text{C}_{\text{DIC}}$ by fixing light DIC, while respiration transfers light OC back to the DIC pool at depth. Such a decrease in $\delta^{13}\text{C}_{\text{DIC}}$ can also be seen in the oxycline of Lake La Alberca between 7 and 10 m.

2106

2107

Influence of methanogenesis in Lake La Alberca de los Espinos

2108

La Alberca shows the least saline/alkaline water column and most peculiar geochemical depth profiles among the four lakes. Notably, its [DIC] and $\delta^{13}\text{C}_{\text{DIC}}$ (the lowest of the studied lakes) increase from the lower metalimnion to the hypolimnion, and further into the first cm of sediment porewaters, with $\delta^{13}\text{C}_{\text{DIC}}$ reaching almost 10 ‰ (Figs. 3; 4). The calculated CO_2 partial pressure (P_{CO_2}) increases downward from slightly less than $1 \times P_{\text{CO}_2\text{-atm}}$ near the lake surface up to almost 40x at the bottom of the lake (Table S2).

2113

While the increase of [POC] at depth may contribute to the observed $\delta^{13}\text{C}_{\text{DIC}}$ increase, by mass balance, it should also lower the [DIC] instead of increasing it. Similarly, the sinking of POC at depth followed by its remineralization into DIC cannot explain these observations since it would lower the $\delta^{13}\text{C}_{\text{DIC}}$ in the hypolimnion (Fig. 4). Overall, these observations require that a significant source of inorganic ^{13}C -rich carbon fuels the bottom waters of La Alberca de los Espinos. The source of heavy carbon most likely results from methanogenesis, which consumes organic carbon in the sediments and produces ^{13}C -depleted methane and ^{13}C -rich carbon dioxide diffusing upward in the water column (i.e. acetoclastic methanogenesis, dominant in lacustrine contexts, Whiticar

2119

Supprimé: (

Supprimé:)

Supprimé: Increase of

Supprimé: residues

Supprimé: Indeed, heterotrophic

Supprimé: In Lake La Preciosa, the water column shifts from a highly oxygenated state to anoxia over a ~5 m interval against more than 10 m for Alchichica and Atexcac. This correlates with a sharp $\delta^{13}\text{C}_{\text{POC}}$ increase (+ 3.4‰), highlighting how efficient and O_2 -dependent the remineralization process is in this lake.

Supprimé: lakes Alchichica and

Mis en forme : Police :Non Italique

Supprimé: of the

Supprimé: Lake

Supprimé: porewaters of the

Supprimé: sediments

Supprimé: up to ~

Supprimé:

Supprimé: Consistently, the

Supprimé: that of atmospheric

Supprimé: S1

Supprimé: those

Supprimé: this

Supprimé: likely

2144 et al., 1986). Methanogenesis, as an “alternative” OM remineralization pathway ~~would~~ be favored in La Alberca,
 2145 because ~~it~~ is relatively rich in OM (notably with high [DOC], Havas et al., submitted), and depleted in SO_4^{2-}
 2146 (Wittkop et al., 2014; Birgel et al., 2015; Cadeau et al., 2020) compared with the three other Mexican lakes. Based
 2147 on the $\delta^{13}\text{C}_{\text{SOC}}$ and porewater $\delta^{13}\text{C}_{\text{DIC}}$, we can tentatively calculate the methane isotopic signature, ~~in La Alberca~~
 2148 (see supplementary text S5). ~~The resulting~~ $\delta^{13}\text{C}_{\text{CH}_4}$ in the first 10 cm of sediments is between -59 and -57 ‰, which
 2149 is consistent with the range of isotopic composition of methane after biogenic methanogenesis (Whiticar et al.,
 2150 1986).

2151 Upward diffusing methane may be either (i) partly lost from the lake’s surface (i.e. escaping the system) by
 2152 degassing or (ii) totally ~~retained~~ in the water column by complete oxidation (either abiotically by oxygenated
 2153 surface waters or biologically by methanotrophic organisms). The oxidation of CH_4 in the water column should
 2154 lead to the formation of ^{13}C -depleted carbon dioxide that would mix back with the lake DIC (and notably with
 2155 heavy methanogenic CO_2 produced at depth) and/or ^{13}C -depleted biomass (as POC or SOC) if it occurs ~~through~~
 2156 methanotrophy. Thus, the net effect of combined methanogenesis and methane oxidation is expected to (i) generate
 2157 a $\delta^{13}\text{C}_{\text{DIC}}$ gradient from high to low values between the sediment porewaters and the oxycline as proposed
 2158 elsewhere (Assayag et al., 2008; Wittkop et al., 2014) and (ii) progressively lower sedimentary $\delta^{13}\text{C}_{\text{SOC}}$ in ~~the~~ case
 2159 of methanotrophy. Abiotic oxidation of methane by dioxygen is consistent with the ~~observation~~ that $\delta^{13}\text{C}_{\text{DIC}}$
 2160 decreases from porewaters (~+10 ‰) to the oxycline (-4 ‰), reaching minimum values where dissolved- O_2 starts
 2161 to appear (Fig. 2). ~~Microbial~~ anaerobic oxidation of methane (AOM) could occur at the 17 m depth through Mn-
 2162 ~~oxide~~ reduction (Cai et al., 2021; Cheng et al., 2021) and possibly bacterial sulfate-reduction closer to the water-
 2163 sediment interface, as inferred for the surficial sediments of meromictic Lake Cadagno (Posth et al., 2017). Indeed,
 2164 we observe a net increase of particulate Fe and S concentrations at a depth of 25 m and a peak of solid sulfide
 2165 minerals in the surficial sediments (Fig. S5). However, $\delta^{13}\text{C}_{\text{SOC}}$ and $\delta^{13}\text{C}_{\text{POC}}$ are far from calculated $\delta^{13}\text{C}_{\text{CH}_4}$,
 2166 suggesting that AOM is not a major process in the bottom lake waters and surface sediments (Lehmann et al.,
 2167 2004) and thus that methanotrophy is not the main CH_4 oxidation pathway in Lake La Alberca.

2168 Alternatively, if some portion of the methane escaped oxidation and degassed out of the lake, $\delta^{13}\text{C}_{\text{DIC}}$ would likely
 2169 be driven to extreme positive values with time (Gu et al., 2004; Hassan, 2014; Birgel et al., 2015; Cadeau et al.,
 2170 2020). This is not consistent with the ~~average~~ $\delta^{13}\text{C}_{\text{DIC}}$ in La Alberca (~~~~~ -3 ‰; Fig. 4), unless an additional
 2171 counterbalancing source of DIC to this lake ~~exists~~. This source of DIC could be volcanic CO_2 -degassing (see
 2172 section 5.1.1). ~~Such a contribution may maintain the lake’s average $\delta^{13}\text{C}_{\text{total}}$ close to a mantle isotopic signature
 2173 and notably away from extreme positive values if CH_4 -escape dominated. It is also possible that volcanic CO_2
 2174 degassing is coupled to methanogenesis by CO_2 reduction in addition to the acetoclastic type described above.~~

2175 Although volcanic CO_2 could be an important source in the C mass balance of Lake La Alberca, we note that it
 2176 cannot explain the very positive $\delta^{13}\text{C}_{\text{DIC}}$ in the sediment porewaters alone, thus bolstering the identification of
 2177 methanogenesis. ~~Importantly, this methane cycle is cryptic to the sediment record, as it is evidenced in the
 2178 dissolved inorganic C phase, but not in the sedimentary organic matter or carbonates. This is a consequence of the
 2179 lake’s stratified nature, where the location of carbonate precipitation and methane production is decoupled.~~

2180 ▲
 2181 *Transfer of OM from the water column to the surficial sediments*

Supprimé: could

Supprimé: Lake

Supprimé: this lake

Supprimé: isotopic compositions of sedimentary organic carbon

Déplacé (insertion) [35]

Supprimé: DIC in Lake La Alberca

Mis en forme : Couleur de police : Automatique

Supprimé: S4

Supprimé: calculated

Mis en forme : Police :Non Italique

Supprimé: kept

Supprimé: by

Supprimé: observations

Supprimé: On the other hand, microbial

Supprimé: oxides

Supprimé: , as observed elsewhere

Supprimé: observation that the

Supprimé: Lake

Supprimé: is about

Supprimé: ‰ (

Supprimé:

Supprimé: exist

Supprimé:). Such a contribution may maintain the lake’s average $\delta^{13}\text{C}_{\text{total}}$ close to a mantle isotopic signature and notably away from extreme positive values if CH_4 -escape dominated. It is also possible that volcanic CO_2 degassing is coupled to methanogenesis by CO_2 reduction in addition to the acetoclastic one described above. We observe a strong pH decline at depth in this lake (mostly below 17 m, Fig. 2) which could be fostered by both the acidic volcanic gases (Pecoraino et al., 2015) and methanogenesis, although other redox and microbial reactions could impact the pH as well (Soetaert et al., 2007).

Supprimé: Only a future quantification of the fluxes of sedimentary methane production, volcanic CO_2 and possible CH_4 efflux out of the lake will help to quantify the peculiar C cycle of Lake La Alberca.

Mis en forme : Police :Non Italique

2217 The OC content in the first 12 cm of the sediment cores from the four lakes ranges from 1 to 13 wt. % (Table S3).
 2218 This appears to be relatively elevated considering the predominantly autochthonous nature of OC and the
 2219 oligotrophic conditions in these lakes (Alcocer et al., 2014; Havas et al., submitted). In Lake Alchichica, the recent
 2220 OC burial flux in the sediment was estimated to represent between 15 and 26 g.yr⁻¹.m⁻² (Alcocer et al., 2014). This
 2221 is within the range of values observed for small lakes around the world (Mulholland and Elwood, 1982; Dean and
 2222 Gorham, 1998; Mendonça et al., 2017), though most of them receive allochthonous OM inputs. Different factors
 2223 can favor the preservation of OM including lower respiration and oxidation rates due to anoxic bottom waters and
 2224 scarce benthic biota and/or high sedimentation rates (Alcocer et al., 2014). Anaerobic respiration clearly occurs in
 2225 the four lakes to some extent, as detailed for La Alberca and as seen in the surficial sediment data of the other
 2226 lakes as well (decreasing δ¹³C_{DIC} in Alchichica, increasing C:N ratio in Atexcac and La Preciosa; Table S3).
 2227 Nonetheless, the anoxic conditions prevailing in the hypolimnion most of the year are significantly more favorable
 2228 to OM preservation than oxic conditions (Sobek et al., 2009; Kuntz et al., 2015). While the yearly mixing oxidizes
 2229 most of the water column during the winter, it also generates a bloom of diatoms which fosters OM production
 2230 (through shuttling up of bio essential nutrient such as N and Si) and development of anoxia (e.g. Adame et al.,
 2231 2008). In Alchichica, the large size of some of the phytoplankton was also suggested to favor OM preservation
 2232 (Adame et al., 2008; Ardiles et al., 2011). Because bacterial sulfate reduction (BSR) is a major remineralization
 2233 pathway in SO₄-rich environments (e.g. Jørgensen, 1982), the low sulfate content in La Alberca probably favors
 2234 the preservation of high TOC in the sediments. Even though, appreciable BSR rates may occur in this lake (see
 2235 discussion above and Fig. S5), similarly to other sulfate-poor environments due to rapid S-cycling (e.g. Vuillemin
 2236 et al., 2016; Friese et al., 2021). Again, a complete mass-balance of these lakes C fluxes will be required to estimate
 2237 their net C emission or sequestration behavior.

2238 Although the nature and geochemical signatures of the OM that deposits in the sediments may vary throughout the
 2239 year, it is interesting to infer from what part(s) of the water column surficial sedimentary OM comes during the
 2240 stratified seasons. In the three lakes from the SOB, δ¹³C_{SOC} and (C:N)_{SOM} signatures of the surficial sedimentary
 2241 OM lie somewhere between POM signatures from the upper water column and from the hypolimnion (Figs. 3, 4).
 2242 More precisely, in Alchichica, the most surficial δ¹³C_{SOC} and (C:N)_{SOM} signatures (-25.7 ‰ and 10.4, respectively)
 2243 are much closer to values recorded in the upper water column (~ -26.5 ‰ and 10.5, respectively), implying that
 2244 the upper oxygenic photosynthesis production is primarily recorded. It is consistent with previous studies
 2245 suggesting that most of the phytoplankton biomass being exported is composed of diatoms (Ardiles et al., 2011).
 2246 In Lake Atexcac, however, δ¹³C_{SOC} and (C:N)_{SOM} signatures (~ -26.8 ‰ and 8, respectively) are closer to values
 2247 recorded in the hypolimnion (~ -26.5 ‰ and 6.5, respectively) suggesting that SOM records mostly the anaerobic
 2248 primary production.

2249 In La Alberca, surficial δ¹³C_{SOC} is markedly more negative (by ~ 2 to 3 ‰) than the deepest and shallowest water
 2250 column values (Fig. 4), but close to what is recorded at the redoxline depth of 17 m. However, the (C:N)_{SOM}
 2251 values are much higher than what is measured anywhere in the water column, which is consistent with OM
 2252 remineralization by sulfate-reduction and methanogenesis in the sediments of this lake. Therefore, OM
 2253 biogeochemical signatures in the surficial sediments of La Alberca could be strongly influenced by early diagenesis
 2254 occurring at the water-sediment interface – despite favorable conditions for OM preservation.

Supprimé: of the four lakes contain varying quantities

Supprimé: between 1 and 13 wt. % (Table 3). This appears to be relatively elevated considering the predominant autochthonous nature of OC and

Supprimé: provided

Supprimé: in section 5.2.2,

Supprimé: 3

Supprimé: In Alchichica, the large size if

Supprimé: In La Alberca the low

Supprimé: content (which is an important electron acceptor for anaerobic respiration)

Supprimé: bottom

Supprimé: from

Supprimé: sediments

Supprimé: in

Supprimé: columns

Supprimé: top

Supprimé: lie

Supprimé:)

Supprimé: Accordingly, it was suggested

Supprimé: was

Supprimé: on the contrary

Supprimé: lie

Supprimé: Lake

Supprimé: are

Supprimé:)

Supprimé: they are

Supprimé: of OM

Supprimé: La Alberca's

Supprimé: Importantly though, methanogenesis/methanotrophy are recorded in the surficial sediments porewaters (notably seen through extremely positive δ¹³C_{DIC}) but not in the solid sediments that show neither very negative δ¹³C_{SOC} nor positive δ¹³C_{carbonates} in the first 10 cm.

2290 Overall, this suggests that OM depositing at the bottom of these stratified lakes ~~does~~ not always record geochemical
 2291 signatures from the same ~~layers~~ of the water columns and can be modified by very early diagenesis. ~~It does~~ not
 2292 necessarily record the signatures of primary production by oxygenic photosynthesis from the upper column. For
 2293 example, in Lake Atexcac, sedimentary OM records ~~primary~~ production by anoxygenic photosynthesis, even
 2294 though POC concentration ~~is highest~~ in the upper water column. ~~This highlights the diversity of geochemical~~
 2295 ~~signatures that can stem from continental environments despite their geographical, geological, and climatic~~
 2296 ~~proximity~~. A deeper understanding of the OM transfer process from water ~~column~~ to ~~sediment~~ will require more
 2297 detailed analyses and comparison of the different OM pigments and molecules and could have strong implications
 2298 for ~~the~~ interpretation of the fossil record in ~~deep~~ anoxic time.

- Supprimé: do
- Supprimé: parts
- Supprimé: Notably, they do
- Supprimé: instead
- Supprimé: was maximum
- Supprimé: columns
- Supprimé: sediments
- Supprimé: the

2300 6. CONCLUSIONS AND SUMMARY

2301 The carbon cycles of four stratified alkaline crater lakes were described and compared based on the concentration
 2302 and isotopic compositions of DIC and POC in the water columns and surficial (~10 cm) sedimentary carbonates
 2303 and organic carbon. ~~Overall our study shows the wide diversity of geochemical signatures found in continental~~
 2304 ~~stratified environments despite similar geological and climatic contexts~~. We identify different regimes of C cycling
 2305 in the four lakes due to different biogeochemical reactions related to slight environmental and ecological
 2306 variations. In more ~~detail~~, we show that:

- Supprimé: of

2307 - External abiotic factors, such as the hydrological regime and the inorganic C sources ~~in~~ the lakes, control
 2308 their alkalinity and thus, the buffering ~~capacity~~ of their waters. In turn, ~~these differences in buffering~~
 2309 ~~capacity constrain variations in pH along the stratified water columns as well as the inorganic C isotope~~
 2310 ~~signatures recorded in the water columns and sediments of the lakes. The $\delta^{13}\text{C}_{\text{carb}}$ reflects the abiotic~~
 2311 ~~factors generating the alkalinity gradient, but it is poorly representative of biological processes in lakes~~
 2312 ~~with high alkalinity. The external environmental factors further impact the C mass balance of the lakes~~
 2313 with probable consequences on their net C-emitting or -sequestering status.

- Supprimé: details
- Supprimé: to
- Supprimé: capacities
- Supprimé: it constrains
- Supprimé: stratification of the
- Supprimé: and
- Supprimé: isotopic
- Supprimé: of the lakes water columns and sediments. Furthermore, it impacts the

2314 - Based on POC and DIC concentrations and isotopic compositions, combined with physico-chemical
 2315 parameters, we are able to identify the activity of oxygenic photosynthesis and aerobic respiration in the
 2316 four ~~lakes~~ studied. Anoxygenic photosynthesis and/or chemoautotrophy are also evidenced in ~~twq~~ of the
 2317 lakes, but their POC and DIC signatures can be equivocal.

- Supprimé: lakes
- Supprimé: some

2318 - Methanogenesis is evidenced in the surficial sediments of the OM-rich Lake La Alberca de los Espinos
 2319 and influences the ~~geochemical signatures lower in the water column~~. However, it is recorded only ~~in~~
 2320 analyses of porewater dissolved species, but not imprinted in the sedimentary archives (~~OM and~~
 2321 carbonates).

- Supprimé: lower water column
- Supprimé: .
- Supprimé: by
- Supprimé: solid
- Supprimé: Last, we observe that the
- Supprimé: largely

2322 - ~~The~~ SOM geochemical signatures of these stratified lakes do not all record the same “biogeochemical
 2323 layers” of the water column (e.g. ~~anaerobic vs. aerobic metabolisms~~), and, ~~in some cases~~, can be ~~greatly~~
 2324 modified by early diagenesis.

- Supprimé: in some cases. Meanwhile, most carbonate phases in bottom lake sediments are in isotopic equilibrium with lake oxyclines, while some might be detrital in origin.

2355 **Author Contributions**

2356 RH and CT designed the study in a project directed by PLG, KB and CT. CT, MI, DJ, DM, RT, PLG and KB
2357 collected the samples on the field. RH carried out the measurements for C data; DJ the physico-chemical parameter
2358 probe measurements and EM provided data for trace and major elements. RH and CT analyzed the data. RH wrote
2359 the manuscript with important contributions of all co-authors.

2360

2361 **Competing Interests**

2362 The authors declare that they have no conflict of interest.

2363

2364 **Disclaimer**

2365

2366 **Acknowledgements**

2367 This work was supported by Agence Nationale de la Recherche (France; ANR Microbialites, grant number ANR-
2368 18-CE02-0013-02). The authors thank Anne-Lise Santoni, Elodie Cognard, Théophile Cocquerez and the GISMO
2369 platform (Biogéosciences, Université Bourgogne Franche-Comté, UMR CNRS 6282, France). We thank Céline
2370 Liorzou and Bleuenn Guéguen for the analyses at the Pôle Spectrométrie Océan (Laboratoire Géo-Océan, Brest,
2371 France) and Laure Cordier for ion chromatography analyses at IPGP (France). We thank Nelly Assayag and Pierre
2372 Cadeau for their help on the AP 2003 at IPGP.

2373

2374 **References**

- 2375 Adame, M.F., Alcocer, J., Escobar, E., 2008. Size-fractionated phytoplankton biomass and its implications for
2376 the dynamics of an oligotrophic tropical lake. *Freshw. Biol.* 53, 22–31. [https://doi.org/10.1111/j.1365-
2377 2427.2007.01864.x](https://doi.org/10.1111/j.1365-2427.2007.01864.x)
- 2378 Alcocer, J., 2021. *Lake Alchichica Limnology*, Springer Nature. ed.
- 2379 Alcocer, J., Ruiz-Fernández, A.C., Escobar, E., Pérez-Bernal, L.H., Oseguera, L.A., Ardiles-Gloria, V., 2014.
2380 Deposition, burial and sequestration of carbon in an oligotrophic, tropical lake. *J. Limnol.* 73.
2381 <https://doi.org/10.4081/jlimnol.2014.783>
- 2382 Anderson, N.John., Stedmon, C.A., 2007. The effect of evapoconcentration on dissolved organic carbon
2383 concentration and quality in lakes of SW Greenland. *Freshw. Biol.* 52, 280–289. [https://doi.org/10.1111/j.1365-
2384 2427.2006.01688.x](https://doi.org/10.1111/j.1365-2427.2006.01688.x)
- 2385 Ardiles, V., Alcocer, J., Vilaclara, G., Oseguera, L.A., Velasco, L., 2012. Diatom fluxes in a tropical,
2386 oligotrophic lake dominated by large-sized phytoplankton. *Hydrobiologia* 679, 77–90.
2387 <https://doi.org/10.1007/s10750-011-0853-7>
- 2388 Armienta, M.A., Vilaclara, G., De la Cruz-Reyna, S., Ramos, S., Cenicerros, N., Cruz, O., Aguayo, A., Arcega-
2389 Cabrera, F., 2008. Water chemistry of lakes related to active and inactive Mexican volcanoes. *J. Volcanol.*
2390 *Geotherm. Res.* 178, 249–258. <https://doi.org/10.1016/j.jvolgeores.2008.06.019>
- 2391 Armstrong-Altrin, J.S., Madhavaraju, J., Sial, A.N., Kasper-Zubillaga, J.J., Nagarajan, R., Flores-Castro, K.,
2392 Rodríguez, J.L., 2011. Petrography and stable isotope geochemistry of the cretaceous El Abra Limestones
2393 (Actopan), Mexico: Implication on diagenesis. *J. Geol. Soc. India* 77, 349–359. [https://doi.org/10.1007/s12594-
2394 011-0042-3](https://doi.org/10.1007/s12594-011-0042-3)
- 2395 Assayag, N., Jézéquel, D., Ader, M., Viollier, E., Michard, G., Prévot, F., Agrinier, P., 2008. Hydrological
2396 budget, carbon sources and biogeochemical processes in Lac Pavin (France): Constraints from $\delta^{18}\text{O}$ of water
2397 and $\delta^{13}\text{C}$ of dissolved inorganic carbon. *Appl. Geochem.* 23, 2800–2816.
2398 <https://doi.org/10.1016/j.apgeochem.2008.04.015>

Mis en forme : Police :Times New Roman

- 2399 Assayag, N., Rivé, K., Ader, M., Jézéquel, D., Agrinier, P., 2006. Improved method for isotopic and quantitative
2400 analysis of dissolved inorganic carbon in natural water samples. *Rapid Commun. Mass Spectrom.* 20, 2243–
2401 2251. <https://doi.org/10.1002/rcm.2585>
- 2402 Bade, D.L., Carpenter, S.R., Cole, J.J., Hanson, P.C., Hesslein, R.H., 2004. Controls of $\delta^{13}\text{C}$ -DIC in lakes:
2403 Geochemistry, lake metabolism, and morphometry. *Limnol. Oceanogr.* 49, 1160–1172.
2404 <https://doi.org/10.4319/lo.2004.49.4.1160>
- 2405 Bekker, A., Holmden, C., Beukes, N.J., Kenig, F., Eglinton, B., Patterson, W.P., 2008. Fractionation between
2406 inorganic and organic carbon during the Lomagundi (2.22–2.1 Ga) carbon isotope excursion. *Earth Planet. Sci.*
2407 *Lett.* 271, 278–291. <https://doi.org/10.1016/j.epsl.2008.04.021>
- 2408 Birgel, D., Meister, P., Lundberg, R., Horath, T.D., Bontognali, T.R.R., Bahniuk, A.M., de Rezende, C.E.,
2409 Vasconcelos, C., McKenzie, J.A., 2015. Methanogenesis produces strong ^{13}C enrichment in stromatolites of
2410 Lagoa Salgada, Brazil: a modern analogue for Palaeo-/Neoproterozoic stromatolites? *Geobiology* 13, 245–266.
2411 <https://doi.org/10.1111/gbi.12130>
- 2412 Briones, E.E., Alcocer, J., Cienfuegos, E., Morales, P., 1998. Carbon stable isotopes ratios of pelagic and littoral
2413 communities in Alchichica crater-lake, Mexico. *Int. J. Salt Lake Res.* 7, 345–355.
2414 <https://doi.org/10.1007/BF02442143>
- 2415 Buchan, A., LeCleir, G.R., Gulvik, C.A., González, J.M., 2014. Master recyclers: features and functions of
2416 bacteria associated with phytoplankton blooms. *Nat. Rev. Microbiol.* 12, 686–698.
2417 <https://doi.org/10.1038/nrmicro3326>
- 2418 Cadeau, P., Jézéquel, D., Le Boulanger, C., Fouilland, E., Le Floch, E., Chaduteau, C., Milesi, V., Guélard, J.,
2419 Sarazin, G., Katz, A., d'Amore, S., Bernard, C., Ader, M., 2020. Carbon isotope evidence for large methane
2420 emissions to the Proterozoic atmosphere. *Sci. Rep.* 10, 18186. <https://doi.org/10.1038/s41598-020-75100-x>
- 2421 Cai, C., Li, K., Liu, D., John, C.M., Wang, D., Fu, B., Fakraee, M., He, H., Feng, L., Jiang, L., 2021. Anaerobic
2422 oxidation of methane by Mn oxides in sulfate-poor environments. *Geology* 49, 761–766.
2423 <https://doi.org/10.1130/G48553.1>
- 2424 Callieri, C., Coci, M., Corno, G., Macek, M., Modenutti, B., Balseiro, E., Bertoni, R., 2013. Phylogenetic
2425 diversity of nonmarine picocyanobacteria. *FEMS Microbiol. Ecol.* 85, 293–301. <https://doi.org/10.1111/1574-6941.12118>
- 2427 Camacho, A., Walter, X.A., Picazo, A., Zopfi, J., 2017. Photoferrotrophy: Remains of an Ancient Photosynthesis
2428 in Modern Environments. *Front. Microbiol.* 08. <https://doi.org/10.3389/fmicb.2017.00323>
- 2429 Carrasco-Núñez, G., Ort, M.H., Romero, C., 2007. Evolution and hydrological conditions of a maar volcano
2430 (Atexcac crater, Eastern Mexico). *J. Volcanol. Geotherm. Res.* 159, 179–197.
2431 <https://doi.org/10.1016/j.jvolgeores.2006.07.001>
- 2432 Chako Tchamabé, B., Carrasco-Núñez, G., Miggins, D.P., Németh, K., 2020. Late Pleistocene to Holocene
2433 activity of Alchichica maar volcano, eastern Trans-Mexican Volcanic Belt. *J. South Am. Earth Sci.* 97, 102404.
2434 <https://doi.org/10.1016/j.jsames.2019.102404>
- 2435 Cheng, C., Zhang, J., He, Q., Wu, H., Chen, Y., Xie, H., Pavlostathis, S.G., 2021. Exploring simultaneous
2436 nitrous oxide and methane sink in wetland sediments under anoxic conditions. *Water Res.* 194, 116958.
2437 <https://doi.org/10.1016/j.watres.2021.116958>
- 2438 Close, H.G., Henderson, L.C., 2020. Open-Ocean Minima in $\delta^{13}\text{C}$ Values of Particulate Organic Carbon in the
2439 Lower Euphotic Zone. *Front. Mar. Sci.* 7, 540165. <https://doi.org/10.3389/fmars.2020.540165>
- 2440 Crowe, S.A., Katsev, S., Leslie, K., Sturm, A., Magen, C., Nomosatryo, S., Pack, M.A., Kessler, J.D., Reeburgh,
2441 W.S., Roberts, J.A., González, L., Douglas Haffner, G., Mucci, A., Sundby, B., Fowle, D.A., 2011. The methane
2442 cycle in ferruginous Lake Matano: Methane cycle in ferruginous Lake Matano. *Geobiology* 9, 61–78.
2443 <https://doi.org/10.1111/j.1472-4669.2010.00257.x>

- 2444 Dean, W.E., Gorham, E., 1998. Magnitude and significance of carbon burial in lakes, reservoirs, and peatlands.
2445 *Geology* 26, 535. [https://doi.org/10.1130/0091-7613\(1998\)026<0535:MASOCB>2.3.CO;2](https://doi.org/10.1130/0091-7613(1998)026<0535:MASOCB>2.3.CO;2)
- 2446 Descolas-Gros, C., Fontungne, M., 1990. Stable carbon isotope fractionation by marine phytoplankton during
2447 photosynthesis. *Plant Cell Environ.* 13, 207–218. <https://doi.org/10.1111/j.1365-3040.1990.tb01305.x>
- 2448 Emrich, K., Ehhalt, D.H., Vogel, J.C., 1970. Carbon isotope fractionation during the precipitation of calcium
2449 carbonate. *Earth Planet. Sci. Lett.* 8, 363–371. [https://doi.org/10.1016/0012-821X\(70\)90109-3](https://doi.org/10.1016/0012-821X(70)90109-3)
- 2450 Ferrari, L., Orozco-Esquivel, T., Manea, V., Manea, M., 2012. The dynamic history of the Trans-Mexican
2451 Volcanic Belt and the Mexico subduction zone. *Tectonophysics* 522–523, 122–149.
2452 <https://doi.org/10.1016/j.tecto.2011.09.018>
- 2453 Fogel, M.L., Cifuentes, L.A., 1993. Isotope Fractionation during Primary Production, in: Engel, M.H., Macko,
2454 S.A. (Eds.), *Organic Geochemistry, Topics in Geobiology*. Springer US, Boston, MA, pp. 73–98.
2455 https://doi.org/10.1007/978-1-4615-2890-6_3
- 2456 Fry, B., 2021. $^{13}\text{C}/^{12}\text{C}$ fractionation by marine diatoms 13.
- 2457 Fry, B., Jannasch, H.W., Molyneaux, S.J., Wirsén, C.O., Muramoto, J.A., King, S., 1991. Stable isotope studies
2458 of the carbon, nitrogen and sulfur cycles in the Black Sea and the Cariaco Trench. *Deep Sea Res. Part Oceanogr.*
2459 *Res. Pap.* 38, S1003–S1019. [https://doi.org/10.1016/S0198-0149\(10\)80021-4](https://doi.org/10.1016/S0198-0149(10)80021-4)
- 2460 Fulton, J.M., Arthur, M.A., Thomas, B., Freeman, K.H., 2018. Pigment carbon and nitrogen isotopic signatures
2461 in euxinic basins. *Geobiology* 16, 429–445. <https://doi.org/10.1111/gbi.12285>
- 2462 Furian, S., Martins, E.R.C., Parizotto, T.M., Rezende-Filho, A.T., Victoria, R.L., Barbiero, L., 2013. Chemical
2463 diversity and spatial variability in myriad lakes in Nhecolândia in the Pantanal wetlands of Brazil. *Limnol.*
2464 *Oceanogr.* 58, 2249–2261. <https://doi.org/10.4319/lo.2013.58.6.2249>
- 2465 Gérard, E., Ménez, B., Couradeau, E., Moreira, D., Benzerara, K., Tavera, R., López-García, P., 2013. Specific
2466 carbonate–microbe interactions in the modern microbialites of Lake Alchichica (Mexico). *ISME J.* 7, 1997–
2467 2009. <https://doi.org/10.1038/ismej.2013.81>
- 2468 Gonzales-Partida, E., Barragan-R, R.M., Nieva-G, D., 1993. Analisis geoquimico-isotopico de las especies
2469 carbonicas del fluido geotermico de Los Humeros, Puebla, México. *Geofis. Int.* 32, 299–309.
- 2470 Gröger, J., Franke, J., Hamer, K., Schulz, H.D., 2009. Quantitative Recovery of Elemental Sulfur and Improved
2471 Selectivity in a Chromium-Reducible Sulfur Distillation. *Geostand. Geanalytical Res.* 33, 17–27.
2472 <https://doi.org/10.1111/j.1751-908X.2009.00922.x>
- 2473 Gu, B., Schelske, C.L., Hodell, D.A., 2004. Extreme ^{13}C enrichments in a shallow hypereutrophic lake:
2474 Implications for carbon cycling. *Limnol. Oceanogr.* 49, 1152–1159. <https://doi.org/10.4319/lo.2004.49.4.1152>
- 2475 Hassan, K.M., 2014. Isotope geochemistry of Swan Lake Basin in the Nebraska Sandhills, USA: Large ^{13}C
2476 enrichment in sediment-calcite records. *Geochemistry* 74, 681–690.
2477 <https://doi.org/10.1016/j.chemer.2014.03.004>
- 2478 Havig, J.R., Hamilton, T.L., McCormick, M., McClure, B., Sowers, T., Wegter, B., Kump, L.R., 2018. Water
2479 column and sediment stable carbon isotope biogeochemistry of permanently redox-stratified Fayetteville Green
2480 Lake, New York, U.S.A. *Limnol. Oceanogr.* 63, 570–587. <https://doi.org/10.1002/lno.10649>
- 2481 Havig, J.R., McCormick, M.L., Hamilton, T.L., Kump, L.R., 2015. The behavior of biologically important trace
2482 elements across the oxic/euxinic transition of meromictic Fayetteville Green Lake, New York, USA. *Geochim.*
2483 *Cosmochim. Acta* 165, 389–406. <https://doi.org/10.1016/j.gca.2015.06.024>
- 2484 Hayes, J.M., Popp, B.N., Takigiku, R., Johnson, M.W., 1989. An isotopic study of biogeochemical relationships
2485 between carbonates and organic carbon in the Greenhorn Formation. *Geochim. Cosmochim. Acta* 53, 2961–
2486 2972. [https://doi.org/10.1016/0016-7037\(89\)90172-5](https://doi.org/10.1016/0016-7037(89)90172-5)

2487 Henkel, J.V., Dellwig, O., Pollehne, F., Herlemann, D.P.R., Leipe, T., Schulz-Vogt, H.N., 2019. A bacterial
2488 isolate from the Black Sea oxidizes sulfide with manganese(IV) oxide. *Proc. Natl. Acad. Sci.* 116, 12153–12155.
2489 <https://doi.org/10.1073/pnas.1906000116>

2490 Hessen, D.O., Anderson, T.R., 2008. Excess carbon in aquatic organisms and ecosystems: Physiological,
2491 ecological, and evolutionary implications. *Limnol. Oceanogr.* 53, 1685–1696.
2492 <https://doi.org/10.4319/lo.2008.53.4.1685>

2493 Hurley, S.J., Wing, B.A., Jasper, C.E., Hill, N.C., Cameron, J.C., 2021. Carbon isotope evidence for the global
2494 physiology of Proterozoic cyanobacteria. *Sci. Adv.* 7, eabc8998. <https://doi.org/10.1126/sciadv.abc8998>

2495 Iniesto, M., Moreira, D., Benzerara, K., Muller, E., Bertolino, P., Tavera, R., López-García, P., 2021a. Rapid
2496 formation of mature microbialites in Lake Alchichica, Mexico. *Environ. Microbiol. Rep.* 13, 600–605.
2497 <https://doi.org/10.1111/1758-2229.12957>

2498 Iniesto, M., Moreira, D., Benzerara, K., Reboul, G., Bertolino, P., Tavera, R., López-García, P., 2022. Planktonic
2499 microbial communities from microbialite-bearing lakes sampled along a salinity-alkalinity gradient. *Limnol.*
2500 *Oceanogr.* lno.12233. <https://doi.org/10.1002/lno.12233>

2501 Iniesto, M., Moreira, D., Reboul, G., Deschamps, P., Benzerara, K., Bertolino, P., Saghaï, A., Tavera, R., López-
2502 García, P., 2021b. Core microbial communities of lacustrine microbialites sampled along an alkalinity gradient.
2503 *Environ. Microbiol.* 23, 51–68. <https://doi.org/10.1111/1462-2920.15252>

2504 Iñiguez, C., Capó-Bauçà, S., Niinemets, Ü., Stoll, H., Aguiló-Nicolau, P., Galmés, J., 2020. Evolutionary trends
2505 in RuBisCO kinetics and their co-evolution with CO₂ concentrating mechanisms. *Plant J.* 101, 897–918.
2506 <https://doi.org/10.1111/tpj.14643>

2507 Javoy, M., Pineau, F., Delorme, H., 1986. Carbon and nitrogen isotopes in the mantle. *Chem. Geol., Isotopes in*
2508 *Geology—Picciotto Volume 57*, 41–62. [https://doi.org/10.1016/0009-2541\(86\)90093-8](https://doi.org/10.1016/0009-2541(86)90093-8)

2509 Jézéquel, D., Michard, G., Viollier, E., Agrinier, P., Albéric, P., Lopes, F., Abril, G., Bergonzini, L., 2016.
2510 Carbon Cycle in a Meromictic Crater Lake: Lake Pavin, France, in: Sime-Ngando, T., Boivin, P., Chapron, E.,
2511 Jezequel, D., Meybeck, M. (Eds.), *Lake Pavin: History, Geology, Biogeochemistry, and Sedimentology of a*
2512 *Deep Meromictic Maar Lake*. Springer International Publishing, Cham, pp. 185–203.
2513 https://doi.org/10.1007/978-3-319-39961-4_11

2514 Jiao, N., Herndl, G.J., Hansell, D.A., Benner, R., Kattner, G., Wilhelm, S.W., Kirchman, D.L., Weinbauer, M.G.,
2515 Luo, T., Chen, F., Azam, F., 2010. Microbial production of recalcitrant dissolved organic matter: long-term
2516 carbon storage in the global ocean. *Nat. Rev. Microbiol.* 8, 593–599. <https://doi.org/10.1038/nrmicro2386>

2517 Karhu, J.A., Holland, H.D., 1996. Carbon isotopes and the rise of atmospheric oxygen. *Geology* 24, 867.
2518 [https://doi.org/10.1130/0091-7613\(1996\)024<0867:CIATRO>2.3.CO;2](https://doi.org/10.1130/0091-7613(1996)024<0867:CIATRO>2.3.CO;2)

2519 Klawonn, I., Van den Wyngaert, S., Parada, A.E., Arandia-Gorostidi, N., Whitehouse, M.J., Grossart, H.-P.,
2520 Dekas, A.E., 2021. Characterizing the “fungal shunt”: Parasitic fungi on diatoms affect carbon flow and bacterial
2521 communities in aquatic microbial food webs. *Proc. Natl. Acad. Sci.* 118, e2102225118.
2522 <https://doi.org/10.1073/pnas.2102225118>

2523 Knossow, N., Blonder, B., Eckert, W., Turchyn, A.V., Antler, G., Kamyshny, A., 2015. Annual sulfur cycle in a
2524 warm monomictic lake with sub-millimolar sulfate concentrations. *Geochem. Trans.* 16, 7.
2525 <https://doi.org/10.1186/s12932-015-0021-5>

2526 Kuntz, L.B., Laakso, T.A., Schrag, D.P., Crowe, S.A., 2015. Modeling the carbon cycle in Lake Matano.
2527 *Geobiology* 13, 454–461. <https://doi.org/10.1111/gbi.12141>

2528 Lehmann, M.F., Bernasconi, S.M., Barbieri, A., McKenzie, J.A., 2002. Preservation of organic matter and
2529 alteration of its carbon and nitrogen isotope composition during simulated and in situ early sedimentary
2530 diagenesis. *Geochim. Cosmochim. Acta* 66, 3573–3584. [https://doi.org/10.1016/S0016-7037\(02\)00968-7](https://doi.org/10.1016/S0016-7037(02)00968-7)

2531 Lehmann, M.F., Bernasconi, S.M., McKenzie, J.A., Barbieri, A., Simona, M., Veronesi, M., 2004. Seasonal
2532 variation of the δC and δN of particulate and dissolved carbon and nitrogen in Lake Lugano: Constraints on

- 2533 biogeochemical cycling in a eutrophic lake. *Limnol. Oceanogr.* 49, 415–429.
2534 <https://doi.org/10.4319/lo.2004.49.2.0415>
- 2535 Lelli, M., Kretzschmar, T.G., Cabassi, J., Doveri, M., Sanchez-Avila, J.I., Gherardi, F., Magro, G., Norelli, F.,
2536 2021. Fluid geochemistry of the Los Humeros geothermal field (LHGF - Puebla, Mexico): New constraints for
2537 the conceptual model. *Geothermics* 90, 101983. <https://doi.org/10.1016/j.geothermics.2020.101983>
- 2538 Li, H.-C., Ku, T.-L., 1997. $\delta^{13}\text{C}$ – $\delta^{18}\text{C}$ covariance as a paleohydrological indicator for closed-basin lakes.
2539 *Palaeogeogr. Palaeoclimatol. Palaeoecol.* 133, 69–80. [https://doi.org/10.1016/S0031-0182\(96\)00153-8](https://doi.org/10.1016/S0031-0182(96)00153-8)
- 2540 Lorenz, V., 1986. On the growth of maars and diatremes and its relevance to the formation of tuff rings. *Bull.*
2541 *Volcanol.* 48, 265–274. <https://doi.org/10.1007/BF01081755>
- 2542 Lugo, A., Alcocer, J., Sánchez, Ma. del R., Escobar, E., Macek, M., 2000. Temporal and spatial variation of
2543 bacterioplankton abundance in a tropical, warm-monomictic, saline lake: Alchichica, Puebla, Mexico. *SIL Proc.*
2544 1922-2010 27, 2968–2971. <https://doi.org/10.1080/03680770.1998.11898217>
- 2545 Lugo, A., Alcocer, J., Sanchez, M.R., Escobar, E., 1993. Trophic status of tropical lakes indicated by littoral
2546 protozoan assemblages. *SIL Proc.* 1922-2010 25, 441–443. <https://doi.org/10.1080/03680770.1992.11900159>
- 2547 Lyons, T.W., Reinhard, C.T., Planavsky, N.J., 2014. The rise of oxygen in Earth's early ocean and atmosphere.
2548 *Nature* 506, 307–315. <https://doi.org/10.1038/nature13068>
- 2549 Macek, M., Medina, X.S., Picazo, A., Peštová, D., Reyes, F.B., Hernández, J.R.M., Alcocer, J., Ibarra, M.M.,
2550 Camacho, A., 2020. Spirostomum teres: A Long Term Study of an Anoxic-Hypolimnion Population Feeding
2551 upon Photosynthesizing Microorganisms. *Acta Protozool.* 59, 13–38.
2552 <https://doi.org/10.4467/16890027AP.20.002.12158>
- 2553 Mason, E., Edmonds, M., Turchyn, A.V., 2017. Remobilization of crustal carbon may dominate volcanic arc
2554 emissions. *Science* 357, 290–294. <https://doi.org/10.1126/science.aan5049>
- 2555 Mendonça, R., Müller, R.A., Clow, D., Verpoorter, C., Raymond, P., Tranvik, L.J., Sobek, S., 2017. Organic
2556 carbon burial in global lakes and reservoirs. *Nat. Commun.* 8, 1694. <https://doi.org/10.1038/s41467-017-01789-6>
- 2557 Mercedes-Martín, R., Ayora, C., Tritlla, J., Sánchez-Román, M., 2019. The hydrochemical evolution of alkaline
2558 volcanic lakes: a model to understand the South Atlantic Pre-salt mineral assemblages. *Earth-Sci. Rev.* 198,
2559 102938. <https://doi.org/10.1016/j.earscirev.2019.102938>
- 2560 Milesi, V.P., Debure, M., Marty, N.C.M., Capano, M., Jézéquel, D., Steefel, C., Rouchon, V., Albéric, P., Bard,
2561 E., Sarazin, G., Guyot, F., Virgone, A., Gaucher, É.C., Ader, M., 2020. Early Diagenesis of Lacustrine
2562 Carbonates in Volcanic Settings: The Role of Magmatic CO₂ (Lake Dziani Dzaha, Mayotte, Indian Ocean).
2563 *ACS Earth Space Chem.* 4, 363–378. <https://doi.org/10.1021/acsearthspacechem.9b00279>
- 2564 Mook, W.G., Bommerson, J.C., Staverman, W.H., 1974. Carbon isotope fractionation between dissolved
2565 bicarbonate and gaseous carbon dioxide. *Earth Planet. Sci. Lett.* 22, 169–176. [https://doi.org/10.1016/0012-821X\(74\)90078-8](https://doi.org/10.1016/0012-821X(74)90078-8)
- 2567 Mulholland, P.J., Elwood, J.W., 1982. The role of lake and reservoir sediments as sinks in the perturbed global
2568 carbon cycle. *Tellus* 34, 490–499. <https://doi.org/10.1111/j.2153-3490.1982.tb01837.x>
- 2569 O'Leary, M.H., 1988. Carbon Isotopes in Photosynthesis. *BioScience* 38, 328–336.
2570 <https://doi.org/10.2307/1310735>
- 2571 Paneth, P., O'Leary, M.H., 1985. Carbon isotope effect on dehydration of bicarbonate ion catalyzed by carbonic
2572 anhydrase. *Biochemistry* 24, 5143–5147. <https://doi.org/10.1021/bi00340a028>
- 2573 Pardue, J.W., Scalan, R.S., Van Baalen, C., Parker, P.L., 1976. Maximum carbon isotope fractionation in
2574 photosynthesis by blue-green algae and a green alga. *Geochim. Cosmochim. Acta* 40, 309–312.
2575 [https://doi.org/10.1016/0016-7037\(76\)90208-8](https://doi.org/10.1016/0016-7037(76)90208-8)
- 2576 Pecoraino, G., D'Alessandro, W., Inguaggiato, S., 2015. The Other Side of the Coin: Geochemistry of Alkaline
2577 Lakes in Volcanic Areas, in: Rouwet, D., Christenson, B., Tassi, F., Vandemeulebrouck, J. (Eds.), *Volcanic*

- 2578 Lakes, *Advances in Volcanology*. Springer Berlin Heidelberg, Berlin, Heidelberg, pp. 219–237.
2579 https://doi.org/10.1007/978-3-642-36833-2_9
- 2580 Peiffer, L., Carrasco-Núñez, G., Mazot, A., Villanueva-Estrada, R.E., Inguaggiato, C., Bernard Romero, R.,
2581 Rocha Miller, R., Hernández Rojas, J., 2018. Soil degassing at the Los Humeros geothermal field (Mexico). *J.*
2582 *Volcanol. Geotherm. Res.* 356, 163–174. <https://doi.org/10.1016/j.jvolgeores.2018.03.001>
- 2583 Petrash, D.A., Steenbergen, I.M., Valero, A., Meador, T.B., Pačes, T., Thomazo, C., 2022. Aqueous system-level
2584 processes and prokaryote assemblages in the ferruginous and sulfate-rich bottom waters of a post-mining lake.
2585 *Biogeosciences* 19, 1723–1751. <https://doi.org/10.5194/bg-19-1723-2022>
- 2586 Pimenov, N.V., Lunina, O.N., Prusakova, T.S., Rusanov, I.I., Ivanov, M.V., 2008. Biological fractionation of
2587 stable carbon isotopes at the aerobic/anaerobic water interface of meromictic water bodies. *Microbiology* 77,
2588 751–759. <https://doi.org/10.1134/S0026261708060131>
- 2589 Posth, N.R., Bristow, L.A., Cox, R.P., Habicht, K.S., Danza, F., Tonolla, M., Frigaard, N. -U., Canfield, D.E.,
2590 2017. Carbon isotope fractionation by anoxygenic phototrophic bacteria in euxinic Lake Cadagno. *Geobiology*
2591 15, 798–816. <https://doi.org/10.1111/gbi.12254>
- 2592 Rendon-Lopez, M.J., 2008. *Limnología física del lago crater los Espinos*, Municipio de Jiménez Michoacan.
- 2593 Ridgwell, A., Arndt, S., 2015. Chapter 1 - Why Dissolved Organics Matter: DOC in Ancient Oceans and Past
2594 Climate Change, in: Hansell, D.A., Carlson, C.A. (Eds.), *Biogeochemistry of Marine Dissolved Organic Matter*
2595 (Second Edition). Academic Press, Boston, pp. 1–20. <https://doi.org/10.1016/B978-0-12-405940-5.00001-7>
- 2596 Sackett, W.M., Eckelmann, W.R., Bender, M.L., Bé, A.W.H., 1965. Temperature Dependence of Carbon Isotope
2597 Composition in Marine Plankton and Sediments. *Science* 148, 235–237.
2598 <https://doi.org/10.1126/science.148.3667.235>
- 2599 Saghaï, A., Zivanovic, Y., Moreira, D., Benzerara, K., Bertolino, P., Ragon, M., Tavera, R., López-Archilla,
2600 A.I., López-García, P., 2016. Comparative metagenomics unveils functions and genome features of microbialite-
2601 associated communities along a depth gradient: Comparative metagenomics of microbialites from Lake
2602 Alchichica. *Environ. Microbiol.* 18, 4990–5004. <https://doi.org/10.1111/1462-2920.13456>
- 2603 Saini, J.S., Hassler, C., Cable, R., Fourquez, M., Danza, F., Roman, S., Tonolla, M., Storelli, N., Jacquet, S.,
2604 Zdobnov, E.M., Duhaime, M.B., 2021. Microbial loop of a Proterozoic ocean analogue (preprint). *Microbiology*.
2605 <https://doi.org/10.1101/2021.08.17.456685>
- 2606 Satkoski, A.M., Beukes, N.J., Li, W., Beard, B.L., Johnson, C.M., 2015. A redox-stratified ocean 3.2 billion
2607 years ago. *Earth Planet. Sci. Lett.* 430, 43–53. <https://doi.org/10.1016/j.epsl.2015.08.007>
- 2608 Schidlowski, M., 2001. Carbon isotopes as biogeochemical recorders of life over 3.8 Ga of Earth history:
2609 evolution of a concept. *Precambrian Res.* 106, 117–134. [https://doi.org/10.1016/S0301-9268\(00\)00128-5](https://doi.org/10.1016/S0301-9268(00)00128-5)
- 2610 Schiff, S.L., Tsuji, J.M., Wu, L., Venkiteswaran, J.J., Molot, L.A., Elgood, R.J., Paterson, M.J., Neufeld, J.D.,
2611 2017. Millions of Boreal Shield Lakes can be used to Probe Archaean Ocean Biogeochemistry. *Sci. Rep.* 7,
2612 46708. <https://doi.org/10.1038/srep46708>
- 2613 Siebe, C., Guilbaud, M.-N., Salinas, S., Chédeville-Monzo, C., 2012. Eruption of Alberca de los Espinos tuff
2614 cone causes transgression of Zacapu lake ca. 25,000 yr BP in Michoacán, México. Presented at the IAS 4IMC
2615 Conference, Auckland, New Zealand, pp. 74–75.
- 2616 Siebe, C., Guilbaud, M.-N., Salinas, S., Kshirsagar, P., Chevrel, M.O., Jiménez, A.H., Godínez, L., 2014.
2617 Monogenetic volcanism of the Michoacán-Guanajuato Volcanic Field: Maar craters of the Zacapu basin and
2618 domes, shields, and scoria cones of the Tarascan highlands (Paracho-Paricutin region). Presented at the Pre-
2619 meeting field guide for the 5th international Maar Conference, Querétaro, México, pp. 1–37.
- 2620 Sigala, I., Caballero, M., Correa-Metrio, A., Lozano-García, S., Vázquez, G., Pérez, L., Zawisza, E., 2017. Basic
2621 limnology of 30 continental waterbodies of the Transmexican Volcanic Belt across climatic and environmental
2622 gradients. *Bol. Soc. Geológica Mex.* 69, 313–370. <https://doi.org/10.18268/BSGM2017v69n2a3>
- 2623 Silva Aguilera, R.A., 2019. Analisis del descenso del nivel de agua del lago Alchichica, Puebla, México 120.

- 2624 Sirevag, R., Buchanan, B.B., Berry, J.A., Troughton, J.H., 1977. Mechanisms of CO₂ Fixation in Bacterial
2625 Photosynthesis Studied by the Carbon Isotope Fractionation Technique. *Arch Microbiol* 112, 4.
- 2626 Sobek, S., Durisch-Kaiser, E., Zurbrügg, R., Wongfun, N., Wessels, M., Pasche, N., Wehrli, B., 2009. Organic
2627 carbon burial efficiency in lake sediments controlled by oxygen exposure time and sediment source. *Limnol.*
2628 *Oceanogr.* 54, 2243–2254. <https://doi.org/10.4319/lo.2009.54.6.2243>
- 2629 Soetaert, K., Hofmann, A.F., Middelburg, J.J., Meysman, F.J.R., Greenwood, J., 2007. The effect of
2630 biogeochemical processes on pH. *Mar. Chem.* 105, 30–51. <https://doi.org/10.1016/j.marchem.2006.12.012>
- 2631 Talbot, M.R., 1990. A review of the palaeohydrological interpretation of carbon and oxygen isotopic ratios in
2632 primary lacustrine carbonates. *Chem. Geol. Isot. Geosci. Sect.* 80, 261–279. [https://doi.org/10.1016/0168-9622\(90\)90009-2](https://doi.org/10.1016/0168-9622(90)90009-2)
- 2634 Thomas, P.J., Boller, A.J., Satagopan, S., Tabita, F.R., Cavanaugh, C.M., Scott, K.M., 2019. Isotope
2635 discrimination by form IC RubisCO from *Ralstonia eutropha* and *Rhodobacter sphaeroides*, metabolically
2636 versatile members of ' *Proteobacteria* ' from aquatic and soil habitats. *Environ. Microbiol.* 21, 72–80.
2637 <https://doi.org/10.1111/1462-2920.14423>
- 2638 Ussiri, D.A.N., Lal, R., 2017. Carbon Sequestration for Climate Change Mitigation and Adaptation. Springer
2639 International Publishing, Cham. <https://doi.org/10.1007/978-3-319-53845-7>
- 2640 Van Mooy, B.A.S., Keil, R.G., Devol, A.H., 2002. Impact of suboxia on sinking particulate organic carbon:
2641 Enhanced carbon flux and preferential degradation of amino acids via denitrification. *Geochim. Cosmochim.*
2642 *Acta* 66, 457–465. [https://doi.org/10.1016/S0016-7037\(01\)00787-6](https://doi.org/10.1016/S0016-7037(01)00787-6)
- 2643 Vilaclara, G., Chávez, M., Lugo, A., González, H., Gaytán, M., 1993. Comparative description of crater-lakes
2644 basic chemistry in Puebla State, Mexico. *SIL Proc.* 1922-2010 25, 435–440.
2645 <https://doi.org/10.1080/03680770.1992.11900158>
- 2646 Vliet, D.M., Meijerfeldt, F.A.B., Dutilh, B.E., Villanueva, L., Sissinghe Damsté, J.S., Stams, A.J.M., Sánchez-
2647 Andrea, I., 2021. The bacterial sulfur cycle in expanding dysoxic and euxinic marine waters. *Environ. Microbiol.*
2648 23, 2834–2857. <https://doi.org/10.1111/1462-2920.15265>
- 2649 Wang, S., Yeager, K.M., Lu, W., 2016. Carbon isotope fractionation in phytoplankton as a potential proxy for
2650 pH rather than for [CO₂(aq)]: Observations from a carbonate lake. *Limnol. Oceanogr.* 61, 1259–1270.
2651 <https://doi.org/10.1002/lno.10289>
- 2652 Werne, J.P., Hollander, D.J., 2004. Balancing supply and demand: controls on carbon isotope fractionation in the
2653 Cariaco Basin (Venezuela) Younger Dryas to present. *Mar. Chem.* 92, 275–293.
2654 <https://doi.org/10.1016/j.marchem.2004.06.031>
- 2655 Whiticar, M.J., Faber, E., Schoell, M., 1986. Biogenic methane formation in marine and freshwater
2656 environments: CO₂ reduction vs. acetate fermentation—Isotope evidence. *Geochim. Cosmochim. Acta* 50, 693–
2657 709. [https://doi.org/10.1016/0016-7037\(86\)90346-7](https://doi.org/10.1016/0016-7037(86)90346-7)
- 2658 Williams, P.M., Gordon, L.I., 1970. Carbon-13: carbon-12 ratios in dissolved and particulate organic matter in
2659 the sea. *Deep Sea Res. Oceanogr. Abstr.* 17, 19–27. [https://doi.org/10.1016/0011-7471\(70\)90085-9](https://doi.org/10.1016/0011-7471(70)90085-9)
- 2660 Wittkop, C., Teranes, J., Lubenow, B., Dean, W.E., 2014. Carbon- and oxygen-stable isotopic signatures of
2661 methanogenesis, temperature, and water column stratification in Holocene siderite varves. *Chem. Geol.* 389,
2662 153–166. <https://doi.org/10.1016/j.chemgeo.2014.09.016>
- 2663 Zeyen, N., Benzerara, K., Beyssac, O., Daval, D., Muller, E., Thomazo, C., Tavera, R., López-García, P.,
2664 Moreira, D., Duprat, E., 2021. Integrative analysis of the mineralogical and chemical composition of modern
2665 microbialites from ten Mexican lakes: What do we learn about their formation? *Geochim. Cosmochim. Acta*
2666 305, 148–184. <https://doi.org/10.1016/j.gca.2021.04.030>
- 2667 Zohary, T., Erez, J., Gophen, M., Berman-Frank, I., Stiller, M., 1994. Seasonality of stable carbon isotopes
2668 within the pelagic food web of Lake Kinneret. *Limnol. Oceanogr.* 39, 1030–1043.
2669 <https://doi.org/10.4319/lo.1994.39.5.1030>

2670 Zyakun, A.M., Lunina, O.N., Prusakova, T.S., Pimenov, N.V., Ivanov, M.V., 2009. Fractionation of stable
2671 carbon isotopes by photoautotrophically growing anoxygenic purple and green sulfur bacteria. *Microbiology* 78,
2672 757–768. <https://doi.org/10.1134/S0026261709060137>
2673